

# GAUSSIAN BEAM METHODS FOR THE SCHRÖDINGER EQUATION WITH DISCONTINUOUS POTENTIALS

SHI JIN, DONGMING WEI, AND DONGSHENG YIN

ABSTRACT. We propose Eulerian and Lagrangian Gaussian beam methods for the Schrödinger equation with discontinuous potentials. At the quantum barriers where the potential is discontinuous, we derive suitable interface conditions to account for quantum scattering information. These scattering interface conditions are then built into the numerical fluxes in the Eulerian level set formulation of the Gaussian beam methods, and are also used in the Lagrangian formulation, including an interface condition for the Hessian matrix. We carry both 1D and 2D numerical examples to verify the accuracy of the method.

## 1. INTRODUCTION

This paper is concerned with the Schrödinger equation of the form

$$i\epsilon\partial_t u^\epsilon(t, \mathbf{x}) = -\frac{\epsilon^2}{2}\Delta u^\epsilon(t, \mathbf{x}) + V(\mathbf{x})u^\epsilon(t, \mathbf{x}), \quad (1.1)$$

with the WKB initial condition

$$u_0(\mathbf{x}) = A_0(\mathbf{x})e^{\frac{i}{\epsilon}S_0(\mathbf{x})}. \quad (1.2)$$

Here  $u^\epsilon$  is the wave function,  $\epsilon > 0$  is the re-scaled Planck constant, and  $V(x)$  is a time-independent potential function. The physical observables can be defined in terms of  $u^\epsilon(t, \mathbf{x})$ :

$$\text{position density} \quad n^\epsilon = |u^\epsilon|^2, \quad (1.3)$$

$$\text{density flux} \quad J^\epsilon = \frac{\epsilon}{2i}(u^\epsilon \nabla \bar{u}^\epsilon - \bar{u}^\epsilon \nabla u^\epsilon), \quad (1.4)$$

$$\text{kinetic energy} \quad E^\epsilon = \frac{\epsilon^2}{2}|\nabla u^\epsilon|^2. \quad (1.5)$$

Generally speaking, the solution to the Schrödinger equation (1.1) is highly oscillatory when the Planck constant  $\epsilon$  is small. Thus, when using numerical approximations, ie. the finite difference method and finite element method, the number of mesh points in each spatial direction should be at least  $o(\epsilon^{-1})$  [29], a typical order with the reasonable meshing strategy. If the potential is sufficiently smooth, and the initial data of the Schrödinger equation is compactly supported, the time-splitting spectral method in [2] was shown to be the best among the existing methods, with number of the spatial meshing points of almost optimal order  $O(\epsilon^{-1})$  in each spatial direction. Unfortunately, this strategy is no longer valid for the Schrödinger equation with non-smooth potentials [15].

---

*Date:* August 30, 2012.

**Acknowledgment.** This work was partially supported by NSF grant DMS- 1114546, and NSF RNMS grant DMS-1107291. SJ was also supported by a Vilas Associate Award from University of Wisconsin-Madison. D. Yin is supported by NSFC grant No. 10901091 and NSFC grant No. 60873252.

One alternative efficient approach for approximating the Schrödinger equation (1.1) is the classical WKB method. For the first order approximation, this method tries to seek an asymptotic solution:

$$u(t, \mathbf{x}) = A(t, \mathbf{x})e^{iS(t, \mathbf{x})/\epsilon} + O(\epsilon), \quad S \in \mathbb{R}, \quad (1.6)$$

where the amplitude  $A$  and the phase  $S$  are smooth functions independent of  $\epsilon$ . Substituting (1.6) into the Schrödinger equation (1.1), one arrives at two equations satisfied by  $S$  and  $A$ :

$$S_t + \frac{1}{2}|\nabla S|^2 + V(\mathbf{x}) = 0, \quad (1.7)$$

$$A_t + \nabla S \cdot \nabla A + \frac{1}{2}\nabla^2 S A = 0. \quad (1.8)$$

The eikonal equation (1.7) is of Hamilton-Jacobi type, which could be solved by the ray tracing method. The amplitude  $A$  is then determined along each specific ray, see [25]. Then the approximate wave function is computed with the expression (1.6).

Despite the tremendous success in handling various wave propagation problems, the classical WKB method has its own shortcomings. A serious drawback is that in general the classical solution to the eikonal equation (1.7) ceases to exist due to the formation of caustics at which points rays intersect and the amplitude  $A$  blows up. Beyond caustics, the correct semiclassical limit to the Schrödinger equation (1.1) contains several phases, namely, the asymptotic solution is actually a sum of functions of the form (1.6). Many approaches have been proposed to resolve this multi-phased solution /or their associated physical observables, such as the big ray tracing method [3], the wave front method [8], the moment method [6, 9, 10, 16], and the level set method [4, 17, 18]. The readers are referred to [7, 14] for reviews of semiclassical computations.

The Gaussian beam method (GB), which was first developed for the Schrödinger equation by Heller in 1970s [11], and independently developed by Popov for linear wave equation [32], is an efficient asymptotic method allows accurate computation of the amplitude near caustics. Similar to the classical ray tracing method, the Gaussian beam solution in physical space also has a WKB form. The rays determined by the Hamiltonian system related to the eikonal equation serve as the centers of the Gaussian beams. The difference lies in that the Gaussian beam allows the phase function to be complex off its center, and the imaginary part of phase function is positive, which makes the solution decay exponentially away from the center. The validity of the Gaussian beam method at caustics was analyzed by Ralston in [34]. This advantage is very important in many applications, for example, in seismic imaging [12, 13]. The uniform convergence was proved by Robert [35] and Liu, Runborg and Tanushev [28] recently.

The accuracy of the beam depends on the truncation error of the Taylor expansion, and the approximate solution is given by a sum of all beams. The accuracy of the Taylor expansion was studied by Motamed and Runborg [30], and Tanushev [39]. Higher order Gaussian beam methods giving better accuracy of the approximation for the linear wave equations were developed and analyzed in [39]. In the 1d Lagrangian formulation, Yin and Zheng [46] constructed a high order Gaussian beam method for the Schrödinger equations and derived the interface conditions for problems with discontinuous potentials. In [37], Tanushev, Engquist and Tsai considered the interface condition of the Gaussian beam method to the wave equation.

The earliest numerical schemes based on the Gaussian beam method were Lagrangian numerical methods. They are based on ray tracing, thus are simple but may lose accuracy when the ray diverges, which will need re-interpolation to maintain a uniform numerical accuracy. The interpolation process can be very complicated. On the other hand, Eulerian methods based on solving PDEs on fixed grids have the advantage of a uniform accuracy. Recently, Eulerian Gaussian beam method has drawn increasing attentions. Based on the work of Tanushev, Qian and Ralston [38], Leung, Qian and Burrige [27] designed an Eulerian Gaussian beam summation method for the Helmholtz equations and the Schrödinger equation [26]. In [21] a new Eulerian Gaussian beam method for the Schrödinger equation using the level set function was derived by Jin, Wu and Yang. A key idea is to construct the Hessian matrix using the partial derivatives of the level set functions. They also extended the Eulerian Gaussian beam method to Schrödinger-Poisson [22] system and use the Bloch decomposition for the Schrödinger equation with periodic potentials [24]. More recently, they introduced Semi-Eulerian and high order Gaussian beam methods for the Schrödinger equation in the semiclassical regime [23]. Another important problem in the Gaussian beam approach is to decompose the initial data into the sum of Gaussian beams, see Tanushev, Engquist and Tsai [37], Ariel, Engquist, Tanushev and Tsai [1], Qian and Ying [33] and Yin and Zheng [47].

In this paper, we extend Gaussian beam methods for the Schrödinger equations to the case of discontinuous potentials in both Eulerian and Lagrangian frameworks in general space dimension. We first derive the interface conditions to account for transmissions and reflections of Gaussian beams at the potential barriers. In particular, the interface conditions for the Hessian matrix is derived which will be used in the Lagrangian formulation. This approach is similar to the high frequency wave propagation in heterogeneous media in [42]. The interface conditions are then combined with the method in [40], which decomposes the partial transmissions and partial reflections into a finite sum of solutions solving problems involving only complete transmissions and complete reflections, and the reinitialization technique for multiple transmissions and reflections. This method allows one to compute the reflections and transmissions across the potential barriers very efficiently.

This paper is organized as follows. The Gaussian beam methods for the Schrödinger equation are sketched in Sect.2. In Sect.3, we derive the interface conditions for Gaussian beam methods at the discontinuous points of the potentials. Formulation and algorithm of Gaussian beam methods with the interface conditions are given in Sect.4. Numerical examples are given in Sect.5 to validate the accuracy of the interface conditions against the full simulation based on solving the original Schrödinger equation. Finally, we make some concluding remarks in Sect.6.

## 2. THE GAUSSIAN BEAM METHODS

In this section, we briefly review the Gaussian beam method for the Schrödinger equation.

**2.1. The Lagrangian dynamics of Gaussian beams.** Similar to the WKB method, the Gaussian beam solution is given in the form

$$\phi_{la}^\epsilon(t, \mathbf{x}, \mathbf{y}_0) = A(t, \mathbf{y})e^{iT(t, \mathbf{x}, \mathbf{y})/\epsilon}, \quad (2.1)$$

where the variable  $\mathbf{y} = \mathbf{y}(t, \mathbf{y}_0)$  is the center of the beam, to be determined below, and the phase  $T(t, \mathbf{x}, \mathbf{y})$  is given by

$$T(t, \mathbf{x}, \mathbf{y}) = S(t, \mathbf{y}) + \mathbf{p}(t, \mathbf{y}) \cdot (\mathbf{x} - \mathbf{y}) + \frac{1}{2}(\mathbf{x} - \mathbf{y})^T M(t, \mathbf{y})(\mathbf{x} - \mathbf{y}).$$

This is reminiscent of the Taylor expansion of the phase  $S$  around the point  $\mathbf{y}$ , upon identifying  $\mathbf{p} = \nabla S \in \mathbb{R}^d$ ,  $M = \nabla^2 S$ , the *Hessian matrix*. The idea is now to allow the phase  $T$  to be complex-valued, and keep the imaginary part of  $M \in \mathbb{C}^{n \times n}$  positive definite so that (2.1) indeed has a Gaussian profile.

Plugging the ansatz (2.1) into the Schrödinger equation (1.1), and ignoring the higher-order terms in both  $\epsilon$  and  $\mathbf{x} - \mathbf{y}$ , one obtains the following system of ODEs:

$$\frac{d\mathbf{y}}{dt} = \mathbf{p}, \quad (2.2)$$

$$\frac{d\mathbf{p}}{dt} = -\nabla_{\mathbf{y}} V, \quad (2.3)$$

$$\frac{dS}{dt} = \frac{1}{2}|\mathbf{p}|^2 - V, \quad (2.4)$$

$$\frac{dM}{dt} = -M^2 - \nabla_{\mathbf{y}}^2 V, \quad (2.5)$$

$$\frac{dA}{dt} = \frac{1}{2}(\text{Tr}(M))A, \quad (2.6)$$

where  $\mathbf{p}, V, M, S$  and  $A$  are functions of  $(t, \mathbf{y}(t, \mathbf{y}_0))$ . Equations (2.2)-(2.3) are the classical Hamiltonian system defining the ray-tracing algorithms. Equations (2.2)-(2.6) define the Lagrangian formulation of the Gaussian beams.

**2.2. The Eulerian dynamics of Gaussian beams.** The Lagrangian Gaussian beam method can be reformulated in an Eulerian framework [21].

Define the linear Liouville operator as

$$\mathcal{L} = \partial_t + \boldsymbol{\xi} \cdot \nabla_{\mathbf{y}} - \nabla_{\mathbf{y}} V \cdot \nabla_{\boldsymbol{\xi}}, \quad (2.7)$$

and denote the level set function

$$\Phi := (\phi_1, \dots, \phi_d).$$

Using the Liouville operator and the level set function, Jin et al. [17] and Jin & Osher [18] showed that one can obtain from the original Lagrangian formulation (2.2)-(2.6) the following Liouville equations for velocity, phase and amplitude, respectively,

$$\mathcal{L}\Phi = 0, \quad (2.8)$$

$$\mathcal{L}S = \frac{1}{2}|\boldsymbol{\xi}|^2 - V, \quad (2.9)$$

$$\mathcal{L}A = \frac{1}{2}\text{Tr}\left((\nabla_{\boldsymbol{\xi}}\Phi)^{-1}\nabla_{\mathbf{y}}\Phi\right)A. \quad (2.10)$$

Note the zero of the real part of  $\Phi$  gives the velocity. In addition, if one introduces the quantity [17],

$$f(t, \mathbf{y}, \boldsymbol{\xi}) = A^2(t, \mathbf{y}, \boldsymbol{\xi}) \det(\nabla_{\boldsymbol{\xi}}\Phi),$$

then  $f(t, \mathbf{y}, \boldsymbol{\xi})$  again satisfies the Liouville equation, i.e.,

$$\mathcal{L}f = 0. \quad (2.11)$$

Then the Eulerian Gaussian beam method is constructed by solving the following Liouville equations

$$\mathcal{L}\Phi = 0, \quad (2.12)$$

$$\mathcal{L}S = \frac{1}{2}|\boldsymbol{\xi}|^2 - V, \quad (2.13)$$

$$\mathcal{L}f = 0. \quad (2.14)$$

The Hessian Matrix  $M$  and amplitude  $A$  are computed by [21]

$$M(t, \mathbf{y}, \boldsymbol{\xi}) = -\nabla_{\mathbf{y}}\Phi(\nabla_{\boldsymbol{\xi}}\Phi)^{-1}, \quad (2.15)$$

$$A(t, \mathbf{y}, \boldsymbol{\xi}) = \left( \det(\nabla_{\boldsymbol{\xi}}\Phi)^{-1} f \right)^{1/2}. \quad (2.16)$$

According to [21], the initial data for (2.12)-(2.14) are given by

$$\Phi(0, \mathbf{y}, \boldsymbol{\xi}) = -i\mathbf{y} + (\boldsymbol{\xi} - \nabla_{\mathbf{y}}S_0(\mathbf{y})), \quad (2.17)$$

$$S(0, \mathbf{y}, \boldsymbol{\xi}) = S_0(\mathbf{y}), \quad (2.18)$$

$$f(0, \mathbf{y}, \boldsymbol{\xi}) = A_0^2(\mathbf{y}). \quad (2.19)$$

The solution to (1.1)-(1.2) is approximated by the following Eulerian Gaussian beam summation formula [21]:

$$u_{GB} = \int_{\mathbb{R}^{2n}} \left( \frac{1}{2\pi\epsilon} \right)^{\frac{n}{2}} r_{\theta}(|\mathbf{x} - \mathbf{y}|) \left( u_{eu}(t, \mathbf{x}, \mathbf{y}, \boldsymbol{\xi}) \prod_{j=1}^n \delta(\operatorname{Re}\phi_j) \right) d\boldsymbol{\xi} d\mathbf{y}, \quad (2.20)$$

where  $r_{\theta} \in C_0^{\infty}(\mathbb{R}^n)$ ,  $r_{\theta} \geq 0$  is a truncation function with  $r_{\theta} \equiv 1$  in a ball of radius  $\theta > 0$  from the origin,  $\delta$  is the Dirac delta function, and

$$u_{eu}(t, \mathbf{x}, \mathbf{y}, \boldsymbol{\xi}) = A(t, \mathbf{y}, \boldsymbol{\xi}) \exp \left( \frac{i}{\epsilon} (S(t, \mathbf{y}) + \mathbf{p}(t, \mathbf{y}) \cdot (\mathbf{x} - \mathbf{y}) + \frac{1}{2}(\mathbf{x} - \mathbf{y})^T M(t, \mathbf{y})(\mathbf{x} - \mathbf{y})) \right).$$

### 3. INTERFACE CONDITIONS

In this section, we give formal derivations of the interface conditions of the Gaussian beams for the Schrödinger equation. For simplicity, we assume that the interface locates at  $y_1 = 0$ . For a more general interface, the argument can be applied in the normal direction. In order to give a simple and clear presentation of the derivation, we assume that the initial wave comes from *the left* of the interface, and hits the interface only *once* (the case of multiple barriers will be treated by the techniques described in subsection 4.2.2). Under this setting, we can decompose the original problem into two parts, one only involves reflection, and the other only involves transmission. Applying the Gaussian beam ansatz, there are two separate systems that correspond to reflected and transmitted beams. We use the Eulerian Gaussian beam formulation to derive the interface conditions for both Eulerian and Lagrangian methods.

We introduce the following notations, see Figure 1:

Region 1 :  $\{\mathbf{y}|y_1 < 0\}$ ,  $\mathbf{y}^- = [0^-, y_2, \dots, y_n]$ ,  $V_1(\mathbf{y}^-) := \lim_{\mathbf{y} \rightarrow \mathbf{y}^-} V_1(\mathbf{y})$ ;

Region 2 :  $\{\mathbf{y}|y_1 > 0\}$ ,  $\mathbf{y}^+ = [0^+, y_2, \dots, y_n]$ .  $V_2(\mathbf{y}^+) := \lim_{\mathbf{y} \rightarrow \mathbf{y}^+} V_2(\mathbf{y})$ ;

transmission set from  $j$  to  $k$  :  $\Xi_t^{j,k} = \left\{ \boldsymbol{\xi} \mid 2(V_j - V_k) + \xi_1^2 > 0 \right\}$ ;

total reflection set from  $j$  to  $k$  :  $\Xi_r^{j,k} = \left\{ \boldsymbol{\xi} \mid 2(V_j - V_k) + \xi_1^2 < 0 \right\}$ ;

the incident wave vector :  $\boldsymbol{\xi}^i := (\xi_1^-, \xi_2, \dots, \xi_n)$ ;

the reflected wave vector :  $\boldsymbol{\xi}^r := (-\xi_1^-, \xi_2, \dots, \xi_n)$ ;

the transmitted wave vector :  $\boldsymbol{\xi}^t := (\xi_1^+, \xi_2, \dots, \xi_n)$ ,

where  $\frac{1}{2}|\boldsymbol{\xi}^t|^2 + V_k = \frac{1}{2}|\boldsymbol{\xi}^i|^2 + V_j$  and  $\xi_1^+ \xi_1^- > 0$ ;

the level set function  $\Phi$  associated with the incident/transmitted/reflected beam :  $\Phi^i/\Phi^t/\Phi^r$ ;

the Hessian matrices of the incident/transmitted/reflected beam :  $M^i/M^t/M^r$ ;

the function  $f$  associated with the incident/transmitted/reflected beam :  $f^i/f^t/f^r$ .

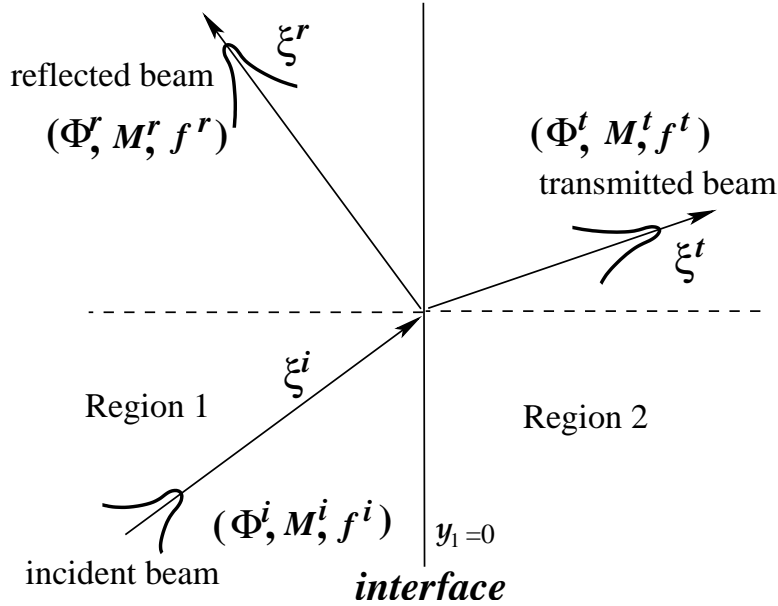


Figure 1: beams at the interface

**3.1. Interface conditions for the reflected beam.** At the interface, we impose the following condition: the level set function  $\Phi$  is continuous along the characteristic, that is

$$\Phi^i(t, \mathbf{y}^-, \boldsymbol{\xi}^i) = \Phi^r(t, \mathbf{y}^-, \boldsymbol{\xi}^r).$$

This implies

$$\nabla_{\mathbf{y}}\Phi^r(t, \mathbf{y}^-, \boldsymbol{\xi}^r) = \nabla_{\mathbf{y}}\Phi^i(t, \mathbf{y}^-, \boldsymbol{\xi}^i), \quad \nabla_{\boldsymbol{\xi}}\Phi^r(t, \mathbf{y}^-, \boldsymbol{\xi}^r) = B\nabla_{\boldsymbol{\xi}}\Phi^i(t, \mathbf{y}^-, \boldsymbol{\xi}^i),$$

where  $B$  is an  $n \times n$  diagonal matrix with  $B_{11} = -1$  and  $B_{mm} = 1$ ,  $m \geq 2$ . Applying the construction of the Hessian  $M = \nabla_{\mathbf{y}}\Phi(\nabla_{\boldsymbol{\xi}}\Phi)^{-1}$ , we obtain the interface condition for the Hessian of reflected beams

$$M^r = -\nabla_{\mathbf{y}}\Phi^r(\nabla_{\boldsymbol{\xi}}\Phi^r)^{-1} = -\nabla_{\mathbf{y}}\Phi^i(\nabla_{\boldsymbol{\xi}}\Phi^i)^{-1}B^{-1} = M^iB. \quad (3.1)$$

This interface condition can be derived by the technique used in [31], which obtained the interface condition for the Gaussian beam method to the wave equation in an inhomogeneous acoustic medium.

By Snell's law, the reflection coefficient  $R$  and the amplitude of the reflected beam  $A^r$  are given by

$$R(\boldsymbol{\xi}^i) = \begin{cases} -1 & \text{if } \boldsymbol{\xi}^i \in \Xi_r^{1,2}, \\ \frac{\xi_1^- - \xi_1^+}{\xi_1^- + \xi_1^+} & \text{otherwise,} \end{cases} \quad (3.2)$$

$$A^r(t, \mathbf{y}^-, \boldsymbol{\xi}^r) = R(\boldsymbol{\xi}^i)A^i(t, \mathbf{y}^-, \boldsymbol{\xi}^i). \quad (3.3)$$

Therefore the interface condition for  $f$  is

$$\begin{aligned} f^r(t, \mathbf{y}^-, \boldsymbol{\xi}^r) &= (A^r)^2(t, \mathbf{y}^-, \boldsymbol{\xi}^r) \det(\nabla_{\boldsymbol{\xi}}\Phi^r(t, \mathbf{y}^-, \boldsymbol{\xi}^r)) \\ &= R^2(\boldsymbol{\xi}^i)(A^i)^2(t, \mathbf{y}^-, \boldsymbol{\xi}^i) \det(B\nabla_{\boldsymbol{\xi}}\Phi^i(t, \mathbf{y}^-, \boldsymbol{\xi}^i)) \\ &= -R^2(\boldsymbol{\xi}^i)(A^i)^2(t, \mathbf{y}^-, \boldsymbol{\xi}^i) \det(\nabla_{\boldsymbol{\xi}}\Phi^i(t, \mathbf{y}^-, \boldsymbol{\xi}^i)) \\ &= -R^2(\boldsymbol{\xi}^i)f^i(t, \mathbf{y}^-, \boldsymbol{\xi}^i). \end{aligned} \quad (3.4)$$

**3.2. Interface conditions for the transmitted beam.** The Liouville equations for  $\Phi^i$  and  $\Phi^t$  are:

$$\partial_t\Phi^i + \boldsymbol{\xi} \cdot \nabla_{\mathbf{y}}\Phi^i - \nabla_{\mathbf{y}}V_1(\mathbf{y}) \cdot \nabla_{\boldsymbol{\xi}}\Phi^i = 0, \quad (3.5a)$$

$$\partial_t\Phi^t + \boldsymbol{\xi} \cdot \nabla_{\mathbf{y}}\Phi^t - \nabla_{\mathbf{y}}V_2(\mathbf{y}) \cdot \nabla_{\boldsymbol{\xi}}\Phi^t = 0. \quad (3.5b)$$

At the interface, we use the condition that  $\Phi$  is continuous along the characteristic, which is

$$\Phi^i(t, \mathbf{y}^-, \boldsymbol{\xi}^i) = \Phi^t(t, \mathbf{y}^+, \boldsymbol{\xi}^t). \quad (3.5c)$$

The conservation of Hamiltonian implies  $V_1(\mathbf{y}^-) + \frac{1}{2}|\boldsymbol{\xi}^i|^2 = V_2(\mathbf{y}^+) + \frac{1}{2}|\boldsymbol{\xi}^t|^2$ . That is

$$V_1(\mathbf{y}^-) + \frac{1}{2}\left((\xi_1^-)^2 + \xi_2^2 + \cdots + \xi_n^2\right) = V_2(\mathbf{y}^+) + \frac{1}{2}\left((\xi_1^+)^2 + \xi_2^2 + \cdots + \xi_n^2\right).$$

Without loss of generality, we assume  $\xi_1^- > 0$ ,  $\xi_1^+ > 0$ , then

$$\xi_1^- = \sqrt{2(V_2(\mathbf{y}^+) - V_1(\mathbf{y}^-)) + (\xi_1^+)^2}.$$

A simple calculation yields:

$$\begin{aligned}
& \partial_{\xi_1} \Phi^t(t, \mathbf{y}^+, \boldsymbol{\xi}^t) \\
&= \lim_{\Delta \xi_1 \rightarrow 0} \frac{1}{\Delta \xi_1} \left[ \Phi^t(t, \mathbf{y}^+, \xi_1^+ + \Delta \xi_1, \xi_2, \dots, \xi_n) - \Phi^t(t, \mathbf{y}^+, \xi_1^+, \xi_2, \dots, \xi_n) \right] \\
&= \lim_{\Delta \xi_1 \rightarrow 0} \frac{1}{\Delta \xi_1} \left[ \Phi^i \left( t, \mathbf{y}^-, \sqrt{2(V_2(\mathbf{y}^+) - V_1(\mathbf{y}^-)) + (\xi_1^+ + \Delta \xi_1)^2}, \xi_2, \dots, \xi_n \right) \right. \\
&\quad \left. - \Phi^i(t, \mathbf{y}^-, \xi_1^-, \xi_2, \dots, \xi_n) \right] = \frac{\xi_1^+}{\xi_1^-} \partial_{\xi_1} \Phi^i(t, \mathbf{y}^-, \boldsymbol{\xi}^i); \\
& \\
& \partial_{\xi_m} \Phi^t(t, \mathbf{y}^+, \boldsymbol{\xi}^t) \qquad \qquad \qquad m \geq 2 \\
&= \lim_{\Delta \xi_m \rightarrow 0} \frac{1}{\Delta \xi_m} \left[ \Phi^t(t, \mathbf{y}^+, \xi_1^+, \dots, \xi_m + \Delta \xi_m, \dots, \xi_n) - \Phi^t(t, \mathbf{y}^+, \xi_1^+, \xi_2, \dots, \xi_n) \right] \\
&= \lim_{\Delta \xi_m \rightarrow 0} \frac{1}{\Delta \xi_m} \left[ \Phi^i \left( t, \mathbf{y}^-, \xi_1^-, \dots, \xi_m + \Delta \xi_m, \dots, \xi_n \right) \right. \\
&\quad \left. - \Phi^i(t, \mathbf{y}^-, \xi_1^-, \xi_2, \dots, \xi_n) \right] = \partial_{\xi_m} \Phi^i(t, \mathbf{y}^-, \boldsymbol{\xi}^i).
\end{aligned}$$

That is,

$$\nabla_{\boldsymbol{\xi}} \Phi^t(t, \mathbf{y}^+, \boldsymbol{\xi}^t) = G(\boldsymbol{\xi}^i) \nabla_{\boldsymbol{\xi}} \Phi^i(t, \mathbf{y}^-, \boldsymbol{\xi}^i). \quad (3.6)$$

Here  $G(\boldsymbol{\xi}^i)$  is an  $n \times n$  matrix with:  $G_{11} = \frac{\xi_1^+}{\xi_1^-}$ ;  $G_{mm} = 1$ ,  $m \geq 2$ .

Next, we derive the interface condition for  $\nabla_{\mathbf{y}} \Phi$ . At the interface  $\Phi^i(t, \mathbf{y}^-, \boldsymbol{\xi}^i) = \Phi^t(t, \mathbf{y}^+, \boldsymbol{\xi}^t)$ , hence

$$\partial_t \Phi^i(t, \mathbf{y}^-, \boldsymbol{\xi}^i) = \partial_t \Phi^t(t, \mathbf{y}^+, \boldsymbol{\xi}^t). \quad (3.7)$$

Combine this with (3.5), we find

$$\begin{aligned}
\left[ \boldsymbol{\xi} \cdot \nabla_{\mathbf{y}} \Phi \right] &\triangleq \boldsymbol{\xi}^t \cdot \nabla_{\mathbf{y}} \Phi^t - \boldsymbol{\xi}^i \cdot \nabla_{\mathbf{y}} \Phi^i \\
&= \nabla_{\mathbf{y}} V_2(\mathbf{y}) \cdot \nabla_{\boldsymbol{\xi}} \Phi^t - \nabla_{\mathbf{y}} V_1(\mathbf{y}) \cdot \nabla_{\boldsymbol{\xi}} \Phi^i \\
&\triangleq \left[ \nabla_{\mathbf{y}} V(\mathbf{y}) \cdot \nabla_{\boldsymbol{\xi}} \Phi \right].
\end{aligned}$$

In the simple case where  $V(\mathbf{y})$  is piecewise constant, the interface condition is reduced to

$$\boldsymbol{\xi}^i \cdot \nabla_{\mathbf{y}} \Phi^i = \boldsymbol{\xi}^t \cdot \nabla_{\mathbf{y}} \Phi^t.$$

Since  $\partial_{y_m} \Phi^i = \partial_{y_m} \Phi^t$  for  $m \geq 2$ , we find a formula for  $\partial_{y_1} \Phi^t$

$$\partial_{y_1} \Phi^t = \frac{\xi_1^-}{\xi_1^+} \partial_{y_1} \Phi^i. \quad (3.8)$$

This yields

$$\nabla_{\mathbf{y}} \Phi^t(t, \mathbf{y}^+, \boldsymbol{\xi}^t) = Q(\boldsymbol{\xi}^i) \nabla_{\mathbf{y}} \Phi^i(t, \mathbf{y}^-, \boldsymbol{\xi}^i).$$

Here  $Q(\boldsymbol{\xi}^i)$  is an  $n \times n$  diagonal matrix with:  $Q_{11} = \frac{\xi_1^-}{\xi_1^+}$ ;  $Q_{mm} = 1$ ,  $m \geq 2$ . Note that  $Q = G^{-1}$ . In the general case, where  $\nabla_{\mathbf{y}}V(\mathbf{y}) \neq 0$ , we have

$$\nabla_{\mathbf{y}}\Phi^t(t, \mathbf{y}^+, \boldsymbol{\xi}^t) = Q(\boldsymbol{\xi}^i)\nabla_{\mathbf{y}}\Phi^i(t, \mathbf{y}^-, \boldsymbol{\xi}^i) + \frac{1}{\xi_1^+}\vec{e}_1 \left[ \nabla_{\mathbf{y}}V(\mathbf{y}) \cdot \nabla_{\boldsymbol{\xi}}\Phi \right]. \quad (3.9)$$

Applying the construction formula of the Hessian

$$M^i = -\nabla_{\mathbf{y}}\Phi^i(\nabla_{\boldsymbol{\xi}}\Phi^i)^{-1}, \quad M^t = -\nabla_{\mathbf{y}}\Phi^t(\nabla_{\boldsymbol{\xi}}\Phi^t)^{-1}, \quad (3.10)$$

combining it with the interface conditions (3.6) and (3.9), we find the interface condition for  $M$

$$\begin{aligned} M^t &= -\left( Q\nabla_{\mathbf{y}}\Phi^i + \frac{1}{\xi_1^+}\vec{e}_1 \left[ \nabla_{\mathbf{y}}V(x) \cdot \nabla_{\boldsymbol{\xi}}\Phi \right] \right) (\nabla_{\boldsymbol{\xi}}\Phi^i)^{-1}Q \\ &= QM^iQ - \frac{1}{\xi_1^+}\vec{e}_1 \left( \nabla_{\mathbf{y}}V_2(\mathbf{y}) \cdot \nabla_{\boldsymbol{\xi}}\Phi^t - \nabla_{\mathbf{y}}V_1(\mathbf{y}) \cdot \nabla_{\boldsymbol{\xi}}\Phi^i \right) (\nabla_{\boldsymbol{\xi}}\Phi^i)^{-1}Q \\ &= QM^iQ - \frac{1}{\xi_1^+}\vec{e}_1 (\nabla_{\mathbf{y}}V_2(\mathbf{y}))^T Q + \frac{1}{\xi_1^+}\vec{e}_1 (\nabla_{\mathbf{y}}V_1(\mathbf{y}))^T Q. \end{aligned} \quad (3.11)$$

**Remark 3.1.** *This interface condition consists of two parts. The first part  $QM^iQ^T$  is due to the jump of the potential. The remaining part is due to the jump of the first derivative of the potential. This interface condition for  $M$  will not be used in the Eulerian computation but will be used in the Lagrangian computation.*

By Snell's law, the transmission coefficient  $T$  and the amplitude of the beam  $A$  are given by

$$T(\boldsymbol{\xi}^i) = \begin{cases} 0 & \text{if } \boldsymbol{\xi}^i \in \Xi_r^{1,2}, \\ \frac{2\xi_1^-}{\xi_1^- + \xi_1^+} & \text{otherwise.} \end{cases} \quad (3.12)$$

$$A^t(t, \mathbf{y}^+, \boldsymbol{\xi}^t) = T(\boldsymbol{\xi}^i)A^i(t, \mathbf{y}^-, \boldsymbol{\xi}^i). \quad (3.13)$$

Similar to the reflected beam, the relation between  $f^t(t, \mathbf{y}^+, \boldsymbol{\xi}^t)$  and  $f^i(t, \mathbf{y}^-, \boldsymbol{\xi}^i)$  is given by

$$\begin{aligned} f^t(t, \mathbf{y}^+, \boldsymbol{\xi}^t) &= (A^t)^2(t, \mathbf{y}^+, \boldsymbol{\xi}^t) \det(\nabla_{\boldsymbol{\xi}}\Phi^t(t, \mathbf{y}^+, \boldsymbol{\xi}^t)) \\ &= T^2(\boldsymbol{\xi}^i)(A^i)^2(t, \mathbf{y}^-, \boldsymbol{\xi}^i) \det(G\nabla_{\boldsymbol{\xi}}\Phi^i(t, \mathbf{y}^-, \boldsymbol{\xi}^i)) \\ &= T^2(\boldsymbol{\xi}^i) \left( \frac{\xi_1^+}{\xi_1^-} \right) (A^i)^2(t, \mathbf{y}^-, \boldsymbol{\xi}^i) \det(\nabla_{\boldsymbol{\xi}}\Phi^i(t, \mathbf{y}^-, \boldsymbol{\xi}^i)) \\ &= T^2(\boldsymbol{\xi}^i) \left( \frac{\xi_1^+}{\xi_1^-} \right) f^i(t, \mathbf{y}^-, \boldsymbol{\xi}^i). \end{aligned} \quad (3.14)$$

**Remark 3.2.** *The Hessian construction formula (3.10) provides advantages in both numerical and analytical aspects. Without the formula (3.10):*

- I. *one has to solve  $2n^2$  more inhomogeneous equations to calculate the Hessian [26];*
- II. *it is hard to proceed when the beam hits the interface because the lack of the interface condition on the Hessian matrix.*

#### 4. FORMULATION AND ALGORITHM

In this section, we formulate the Lagrangian and Eulerian Gaussian beam methods for the Schrödinger equation (1.1) with *discontinuous* potentials.

**4.1. The Lagrangian formulation.** We apply interface conditions (3.1) and (3.11) to construct the Lagrangian Gaussian beam method. Whenever the  $\mathbf{y}$ -trajectory of a beam hits the interface, the beam splits into two beams. We denote the hitting time by  $t_c$ ,  $\mathbf{p}(t_c^-)$  by  $\boldsymbol{\xi}^i$ , and everything associated with the reflected/transmitted beam by  $\{\cdot\}^{r,t}$ . After hitting the interface, the reflected beam at  $t_c^+$  are given by

$$\mathbf{y}^r(t_c^+) = \mathbf{y}(t_c^-), \quad (4.1a)$$

$$A^r(t_c^+) = R(\boldsymbol{\xi}^i)A(t_c^-) \quad (4.1b)$$

$$S^r(t_c^+) = S(t_c^-), \quad (4.1c)$$

$$\mathbf{p}^r(t_c^+) = \boldsymbol{\xi}^r, \quad (4.1d)$$

$$M^r(t_c^+) = M(t_c^-)B. \quad (4.1e)$$

For the transmitted beam, one proceeds in time with the following initial condition

$$\mathbf{y}^t(t_c^+) = \mathbf{y}(t_c^-), \quad (4.2a)$$

$$A^t(t_c^+) = T(\boldsymbol{\xi}^i)A(t_c^-) \quad (4.2b)$$

$$S^t(t_c^+) = S(t_c^-), \quad (4.2c)$$

$$\mathbf{p}^t(t_c^+) = \boldsymbol{\xi}^t, \quad (4.2d)$$

$$M^t(t_c^+) = QM(t_c^-)Q - \frac{1}{\xi_1^+} \vec{e}_1 (\nabla_{\mathbf{y}} V_2(\mathbf{y}))^T Q + \frac{1}{\xi_1^+} \vec{e}_1 (\nabla_{\mathbf{y}} V_1(\mathbf{y}))^T Q. \quad (4.2e)$$

**4.2. The Eulerian Formulation.** The construction of our Eulerian formulation is a combination of the interface condition and the technique proposed in [40]. An earlier level set approach to handle reflection can be found in [5]. We first give the method in a simple situation, where the initial wave comes from the left and hits interface only once. In this case, we decompose the problem into two parts: the reflected part and the transmitted part. The Hessian function, phase and amplitude for the two parts are solved by the Liouville equations (2.12), (2.13) and (2.14) respectively. The fluxes at the interface are connected by proper reflection and transmission conditions given in the proceeding section. Details for the evolution of  $\Phi$ ,  $S$  and  $f$  are given below.

The level set functions  $\Phi^r, \Phi^t$  are obtained by solving the following Liouville equations with the corresponding interface condition at  $y_1 = 0$ ,

$$\begin{cases} \mathcal{L}\Phi^r(t, \mathbf{y}, \boldsymbol{\xi}) = 0, \\ \Phi^r(0, \mathbf{y}, \boldsymbol{\xi}) = -i\mathbf{y} + (\boldsymbol{\xi} - \nabla_{\mathbf{y}} S_0), \\ \Phi^r(t, \mathbf{y}^-, \boldsymbol{\xi}^i) \Big|_{y_1=0} = \Phi^r(t, \mathbf{y}^-, \boldsymbol{\xi}^r) \Big|_{y_1=0}, \end{cases} \quad (4.3a)$$

$$\begin{cases} \mathcal{L}\Phi^t(t, \mathbf{y}, \boldsymbol{\xi}) = 0, \\ \Phi^t(0, \mathbf{y}, \boldsymbol{\xi}) = -i\mathbf{y} + (\boldsymbol{\xi} - \nabla_{\mathbf{y}} S_0), \\ \Phi^t(t, \mathbf{y}^+, \boldsymbol{\xi}^t) \Big|_{y_1=0} = I_{\boldsymbol{\xi}^i \in \Xi_{tr}^{1,2}} \Phi^t(t, \mathbf{y}^-, \boldsymbol{\xi}^i) \Big|_{y_1=0}, \end{cases} \quad (4.3b)$$

where  $I$  is the characteristic function, which is used to capture the beams that are transmitted.

The phase functions and  $f$  satisfy

$$\begin{cases} \mathcal{L}S^r(t, \mathbf{y}, \boldsymbol{\xi}) = \frac{1}{2}|\boldsymbol{\xi}|^2 - V(\mathbf{y}), \\ S^r(0, \mathbf{y}, \boldsymbol{\xi}) = S_0(\mathbf{y}), \\ S^r(t, \mathbf{y}^-, \boldsymbol{\xi}^i) \Big|_{y_1=0} = S^r(t, \mathbf{y}^-, \boldsymbol{\xi}^r) \Big|_{y_1=0}, \end{cases} \quad (4.4a)$$

$$\begin{cases} \mathcal{L}S^t(t, \mathbf{y}, \boldsymbol{\xi}) = \frac{1}{2}|\boldsymbol{\xi}|^2 - V(\mathbf{y}), \\ S^t(0, \mathbf{y}, \boldsymbol{\xi}) = S_0(\mathbf{y}), \\ S^t(t, \mathbf{y}^+, \boldsymbol{\xi}^t) \Big|_{y_1=0} = I_{\boldsymbol{\xi}^i \in \Xi_{tr}^{1,2}} S^t(t, \mathbf{y}^-, \boldsymbol{\xi}^i) \Big|_{y_1=0}, \end{cases} \quad (4.4b)$$

$$\begin{cases} \mathcal{L}f^r(t, \mathbf{y}, \boldsymbol{\xi}) = 0, \\ f^r(0, \mathbf{y}, \boldsymbol{\xi}) = A_0^2(\mathbf{y}), \\ f^r(t, \mathbf{y}^-, \boldsymbol{\xi}^i) \Big|_{y_1=0} = -R^2(\boldsymbol{\xi}^i) f^r(t, \mathbf{y}^-, \boldsymbol{\xi}^r) \Big|_{y_1=0}, \end{cases} \quad (4.5a)$$

$$\begin{cases} \mathcal{L}f^t(t, \mathbf{y}, \boldsymbol{\xi}) = 0, \\ f^t(0, \mathbf{y}, \boldsymbol{\xi}) = S_0(\mathbf{y}), \\ f^t(t, \mathbf{y}^+, \boldsymbol{\xi}^t) \Big|_{y_1=0} = T^2(\boldsymbol{\xi}^i) \frac{\xi_1^+}{\xi_1^-} I_{\boldsymbol{\xi}^i \in \Xi_{tr}^{1,2}} f^t(t, \mathbf{y}^-, \boldsymbol{\xi}^i) \Big|_{y_1=0}. \end{cases} \quad (4.5b)$$

4.2.1. **Algorithm.** The numerical procedure is given as follows:

- Step 1. Solve (4.3a)-(4.5b) with the interface conditions built into the numerical fluxes as in [19].
- Step 2. Compute the Hessian function using the formulation (2.15) and the amplitude from formulation (2.16).
- Step 3. Evaluate the summation integral  $u_{GB}^r$  and  $u_{GB}^t$  (formula (2.20)) by numerically discretizing the delta function using the techniques given in [43, 44, 45]. The solution of the original problem is  $u_{GB} = u_{GB}^r + I_{\{y_1>0\}} u_{GB}^t$ .

4.2.2. **A decomposition method.** Since (2.20) involves the Dirac-delta function, it is valid without interface, or for the case of complete transmission or reflection [20]. In order to deal with partial transmission or reflection, to construct an Eulerian method, one has to separate the level set functions to get the correct information of incident, transmitted and reflected beams. We follow the idea proposed in [40]. It consists of two steps: (i) decompose the original problem into finite many parts where the number of parts only depends on the geometry of the interface, each part is a complete reflection or transmission problem; (ii) reinitialize the problem frequently to capture and separate beams that hit the interface more than once.

For reader's convenience, we briefly describe the decomposition technique for a problem with one interface at  $y_1 = 0$ . For details of problems with more than one interfaces, and details of reinitialization technique, see [40]. Assume every single beam will only intersect the interface at most once in the time interval  $[0, \tau]$ , we solve three problems subject to different initial data and interface conditions. We denote the level set function, the phase and amplitudes of these three problems by  $\Phi^{r,t_1,t_2}$ ,  $S^{r,t_1,t_2}$  and  $f^{r,t_1,t_2}$  respectively, then the initial data and interface

conditions for them are

$$\begin{aligned}
(\Phi_0^r, S_0^r) &= (\Phi_0^{t_1}, S_0^{t_1}) = (\Phi_0^{t_2}, S_0^{t_2}) = (\Phi_0, S_0), \\
f_0^r(\mathbf{y}) &= f_0(\mathbf{y}), \quad f_0^{t_1}(\mathbf{y}) = I_{\{y_1 < 0\}} f_0(\mathbf{y}), \quad f_0^{t_2}(\mathbf{y}) = I_{\{y_1 \geq 0\}} f_0(\mathbf{y}), \\
(\Phi^r, S^r)(t, \mathbf{y}^+, \boldsymbol{\xi}^t) &= (\Phi^r, S^r)(t, \mathbf{y}^+, \boldsymbol{\xi}^r), \quad f^r(t, \mathbf{y}^+, \boldsymbol{\xi}^t) = -R^2(\boldsymbol{\xi}^t) f^r(t, \mathbf{y}^+, \boldsymbol{\xi}^r), \quad \xi_1^+ \geq 0, \\
(\Phi^r, S^r)(t, \mathbf{y}^-, \boldsymbol{\xi}^i) &= (\Phi^r, S^r)(t, \mathbf{y}^-, \boldsymbol{\xi}^r), \quad f^r(t, \mathbf{y}^-, \boldsymbol{\xi}^i) = -R^2(\boldsymbol{\xi}^i) f^r(t, \mathbf{y}^-, \boldsymbol{\xi}^r), \quad \xi_1^- \leq 0, \\
(\Phi^{t_1}, S^{t_1})(t, \mathbf{y}^+, \boldsymbol{\xi}^t) &= (\Phi^{t_1}, S^{t_1})(t, \mathbf{y}^-, \boldsymbol{\xi}^i), \quad f^{t_1}(t, \mathbf{y}^+, \boldsymbol{\xi}^t) = T^2(\boldsymbol{\xi}^t) \frac{\xi_1^-}{\xi_1^+} f^{t_1}(t, \mathbf{y}^-, \boldsymbol{\xi}^i), \quad \xi_1^+ \geq 0, \\
(\Phi^{t_1}, S^{t_1})(t, \mathbf{y}^-, \boldsymbol{\xi}^i) &= (\Phi^{t_1}, S^{t_1})(t, \mathbf{y}^+, \boldsymbol{\xi}^t), \quad f^{t_1}(t, \mathbf{y}^-, \boldsymbol{\xi}^i) = T^2(\boldsymbol{\xi}^i) \frac{\xi_1^+}{\xi_1^-} f^{t_1}(t, \mathbf{y}^+, \boldsymbol{\xi}^t), \quad \xi_1^- \leq 0, \\
(\Phi^{t_2}, S^{t_2})(t, \mathbf{y}^+, \boldsymbol{\xi}^t) &= (\Phi^{t_2}, S^{t_2})(t, \mathbf{y}^-, \boldsymbol{\xi}^i), \quad f^{t_2}(t, \mathbf{y}^+, \boldsymbol{\xi}^t) = T^2(\boldsymbol{\xi}^t) \frac{\xi_1^-}{\xi_1^+} f^{t_2}(t, \mathbf{y}^-, \boldsymbol{\xi}^i), \quad \xi_1^+ \geq 0, \\
(\Phi^{t_2}, S^{t_2})(t, \mathbf{y}^-, \boldsymbol{\xi}^i) &= (\Phi^{t_2}, S^{t_2})(t, \mathbf{y}^+, \boldsymbol{\xi}^t), \quad f^{t_2}(t, \mathbf{y}^-, \boldsymbol{\xi}^i) = T^2(\boldsymbol{\xi}^i) \frac{\xi_1^+}{\xi_1^-} f^{t_2}(t, \mathbf{y}^+, \boldsymbol{\xi}^t), \quad \xi_1^- \leq 0.
\end{aligned}$$

Denote the Gaussian beam solutions corresponding to these three problems by  $u_{GB}^{r,t_1,t_2}$ , then the Gaussian beam solution of the full problem is

$$u_{GB} = u_{GB}^r + I_{\{y_1 \geq 0\}} u_{GB}^{t_1} + I_{\{y_1 < 0\}} u_{GB}^{t_2}, \quad 0 \leq t \leq \tau. \quad (4.6)$$

Here  $I_{\{y_1 \geq 0\}} u_{GB}^{t_1}$  captures the transmitted beams coming from the left,  $I_{\{y_1 < 0\}} u_{GB}^{t_2}$  captures the transmitted beams coming from the right, and  $u_{GB}^r$  captures the reflected beams and beams that haven't hit the interface yet.

## 5. NUMERICAL EXAMPLES

In this section, we give numerical examples to verify the interface conditions and the numerical method. The decomposition and reinitialization techniques proposed in [40] have been applied to these examples.

**Example 5.1.** *Consider the Schrödinger equation*

$$\begin{aligned}
i\epsilon \frac{\partial u}{\partial t} &= -\frac{\epsilon^2}{2} \Delta_x u + V(x)u, \\
u(x, 0) &= A_0(x) e^{iS_0(x)/\epsilon},
\end{aligned}$$

with

$$A_0(x) = \exp(-50 * (x + 0.2)^2), \quad S_0(x) = 1.6x, \quad V(x) = \begin{cases} 0, & x < 0.2, \\ 1, & x > 0.2, \end{cases}$$

In this example, the potential  $V(x)$  contains a single discontinuity at  $x = 0.2$ , thus one needs the interface condition to connect the reflected and transmitted GBs to the incident GB.

For the sake of comparison, a reference solution for the Schrödinger equation is computed by the characteristic expansion method as in [46].

Figure 2(a) shows the wave functions obtained by a direct simulation of the Schrödinger equation and our Gaussian beam summation method. In our computation, the mesh size of the Gaussian beam method is  $\Delta x = 1/256$ , and the time step is chosen to be  $\Delta t = \frac{1}{2}\Delta x$ . When an incident wave hits the potential barrier, it splits into a reflected wave and a transmitted

wave. Coupled with the interface conditions, the GB method captures the reflected wave and a transmitted wave correctly.

Figure 2(b), Figure 2(c) and Figure 2(d) give the comparison of the position density, density flux and kinetic energy respectively between the reference solutions and the solutions by our Gaussian beam method. One can see that our Gaussian beam summation method can capture the physical observables very accurately.

Figure 3 shows the  $l^1$  and  $l^2$  errors between the solution of the direct simulation of the Schrödinger equation and the solution computed by the GB method at time  $t = 0.4$ , where the mesh size  $\Delta x = 1/256$  and the time step  $\Delta t = 1/512$ . The convergence rate of the error in  $\epsilon$  is first order in  $l^1$  and  $l^2$  norms, which is higher than the error estimate of the Gaussian beam solutions for the Schrödinger equation in [28], This is due to error cancellations between adjacent beams as analyzed in [30].

**Example 5.2.** *Consider*

$$\begin{aligned} V(x) &= \begin{cases} 0, & x < 0.4, \\ 0.1 & x > 0.4 \end{cases} \\ A_0(x) &= \exp(-50x^2), \\ S_0(x) &= -0.2 \log(2 \cosh(5x)). \end{aligned}$$

In this example, the semiclassical limit of the Schrödinger equation will develop a cusp caustic. The potential  $V(x)$  is discontinuous at  $x = 0.4$ . We want to test the accuracy of the Gaussian beam method at caustics and the interface conditions.

In Figure 4(a), we compare the wave functions of the reference solution and of the Gaussian beam method for time  $t = 1.2$  and  $1.5$ . One can see that the wave functions are highly oscillatory, and at the sampling point, the error of the Gaussian beam method is very small. This verifies the validity of our interface conditions and the accuracy of the Gaussian beamsolutions near the caustics. Figure 4(b) is the position density of the reference solution and the Gaussian beam summation method, which shows a good agreement. The error of the density flux is shown in Figure 4(c).

In Figure 5, we show the evolution of the wave functions of the reference solution and of our Gaussian beam summation method. There is a cusp caustic at time  $t = 0.2$  and near  $x = 0$ . When the wave hits the potential barrier, there will generate a reflected wave and a transmitted wave. Our method can capture the caustic, the reflection and transmission at the potential barrier.

In Figure 6, we show the convergence rate with respect to  $\epsilon$  for the wave function and position density compared to the reference solution. In this computation, the mesh size  $\Delta x = 1/512$  and the time step is  $\Delta t = 1/1024$ . The convergence rate is first order in both  $l^1$  and  $l^2$  norms.

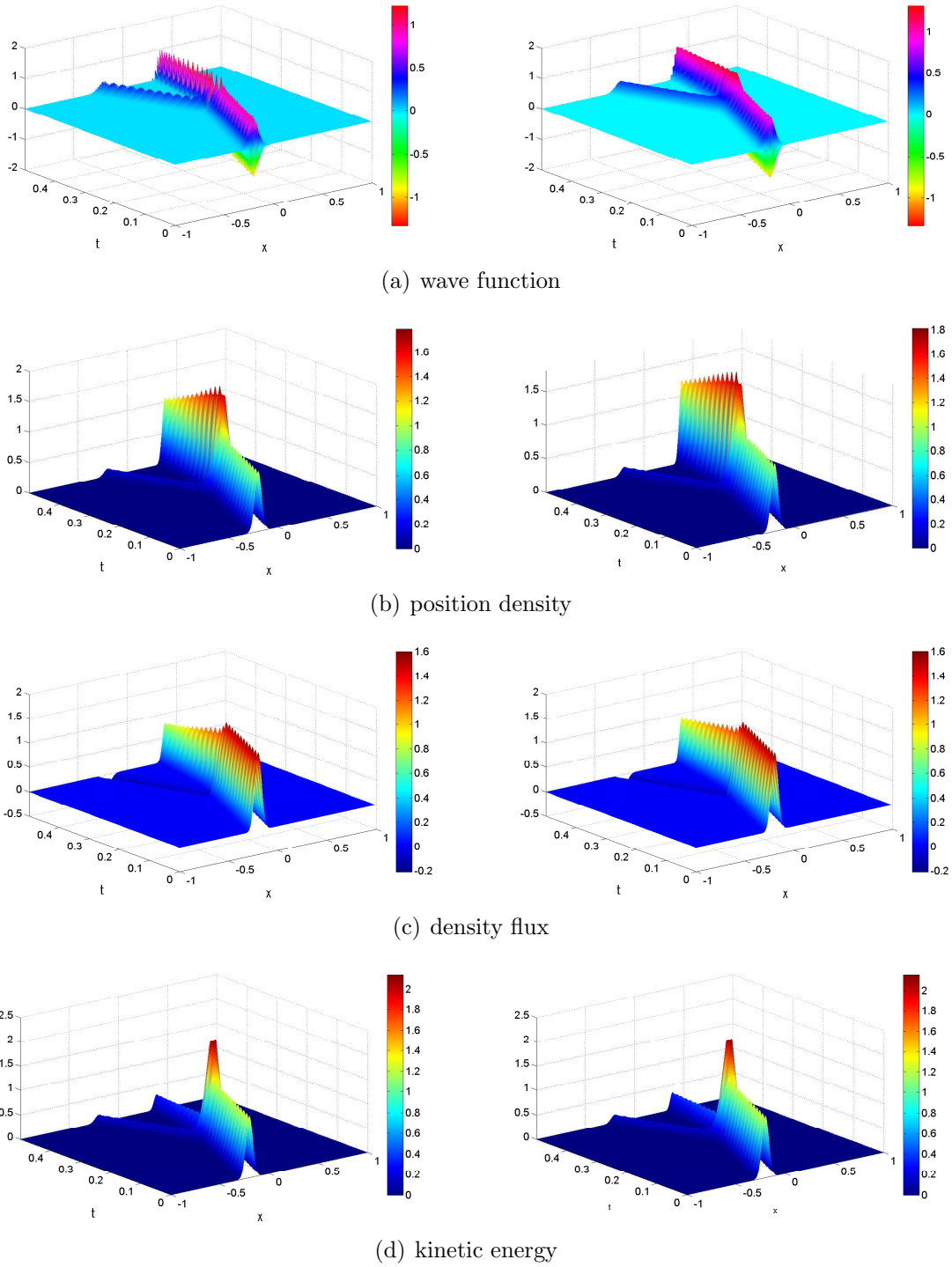


Figure 2: Example 1. The evolution of the wave function with  $\epsilon = 1/500$ : left, the reference solution, right, the approximate solution by GB method.

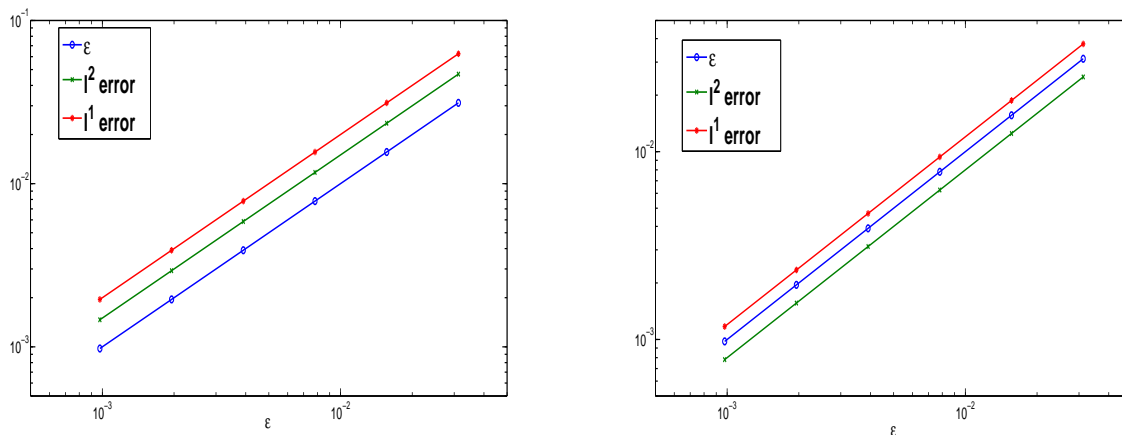


Figure 3: Example 1: the convergence rate with respect to  $\epsilon$  of the  $l^1$  and  $l^2$ . Left, wave function; Right, position density.

**Example 5.3.** Consider  $\epsilon = 1/400$ ,

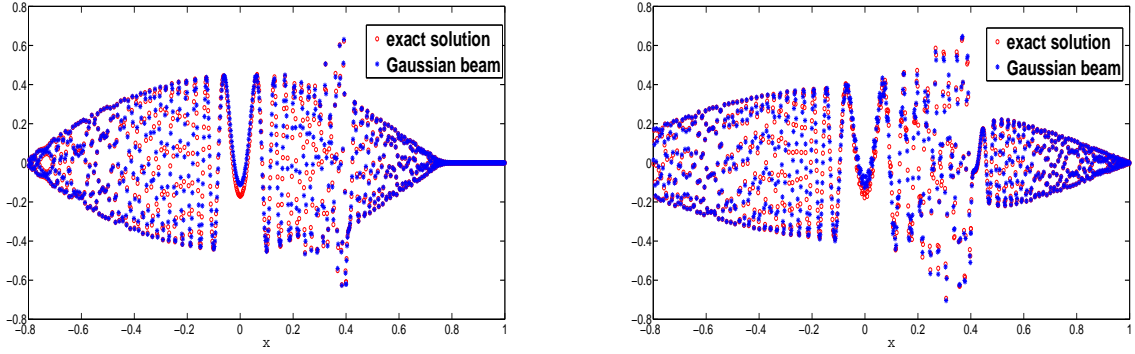
$$A_0(x) = \exp(-100 * (x + 0.4)^2),$$

$$S_0(x) = 1.8x, V(x) = \begin{cases} 0, & x < 0, \\ 1 - 0.2x, & 0 < x < 0.5, \\ -0.2x, & 0.5 < x < 1.5, \\ 1 - 0.2x, & 1.5 < x < 2, \\ -0.5, & x > 2. \end{cases}$$

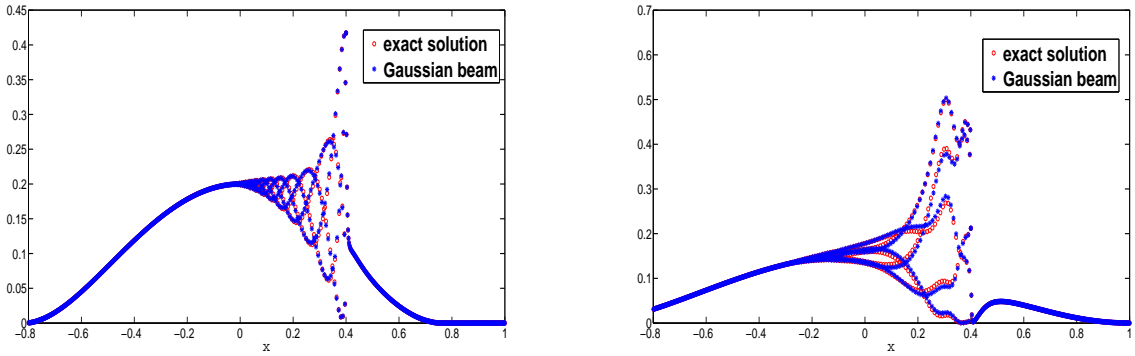
This potential appears in the resonant-tunneling diode (RTD) in nanostructure [36]. Figure 7 shows a diagram of the electric potential within the RTD. In this case, the potential  $V(x)$  contains many discontinuous points, and there will be multi-reflections and transmissions between the potential barriers. If one uses the Lagrangian Gaussian beam method to simulate the Schrödinger equation, the number of the Gaussian beams will grow exponentially due to the multi-reflections and transmissions. We take the mesh size  $\Delta x = 1/512$ , and the time step is chosen to be  $\Delta t = 1/1024$ . Figure 8(a) shows the comparison of the time evolution of the wave functions between the reference solution and the Gaussian beam solution. Figure 8(b) shows the position density of the reference solution and the solution computed by our Gaussian beam method. Our method captures correctly the multi-reflected waves and multi-transmitted waves.

Figure 8(c) and Figure 8(d) give respectively the density flux and kinetic energy for the reference solution and our Gaussian beam method. Our Gaussian beam method can simulate all reflection and transmission accurately.

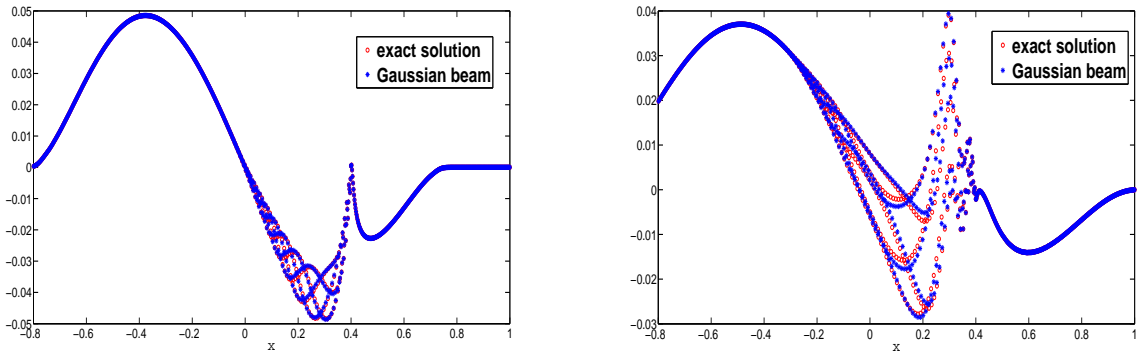
Figure 9 gives the  $l^1$  and  $l^2$  errors between the reference solution and the solution obtained by the Gaussian beam method at time  $t = 1.8$ , where the mesh size  $\Delta x = 1/1024$  and the time step  $\Delta t = 1/2048$ . The convergence rate of the error in  $\epsilon$  is about first order in  $l^1$  and  $l^2$  norms.



(a) wave function



(b) position density



(c) density flux

Figure 4: Example 2: comparison between the reference solution and the solutions by the Gaussian beam method with interface condition. Left, time  $t = 1.2$ , right, time  $t = 1.5$ .

**Example 5.4.** We consider the 2-D Schrödinger equation with  $\epsilon = 1/400$ , where

$$A_0(x, y) = \exp(-100((x + 0.5)^2 + y^2)), \quad S_0(x, y) = 1.5x, \quad V(x, y) = \begin{cases} 0, & x < 0, \\ 1, & x > 0. \end{cases}$$

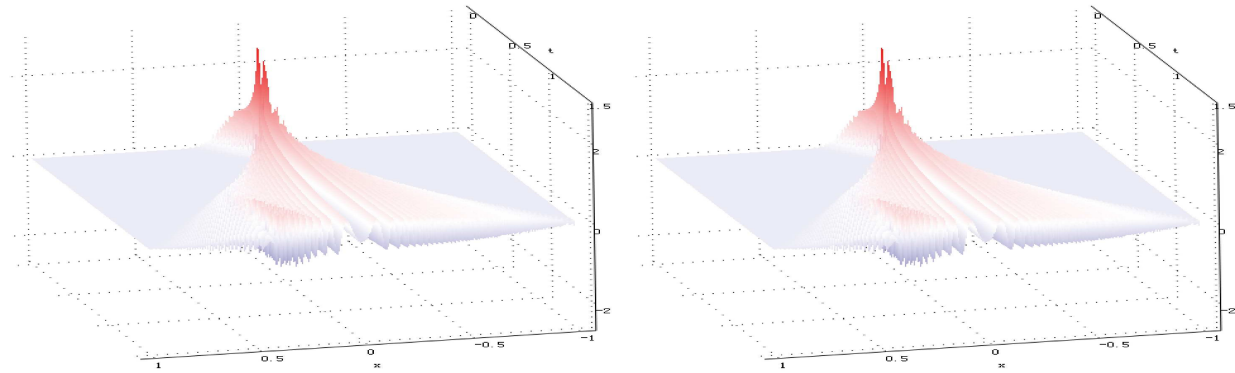


Figure 5: Example 2: the evolution of the wave function, left, the solution of Schrödinger equation, right, solution by the Gaussian beam method with interface condition.

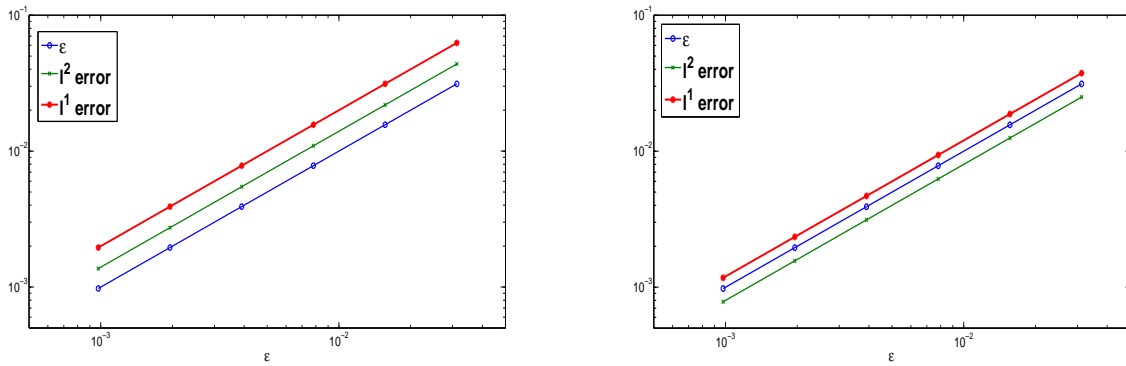


Figure 6: Example 2: the convergence rate with respect to  $\epsilon$  in  $l^1$  and  $l^2$ -norms respectively. Left, wave function; Right, position density.

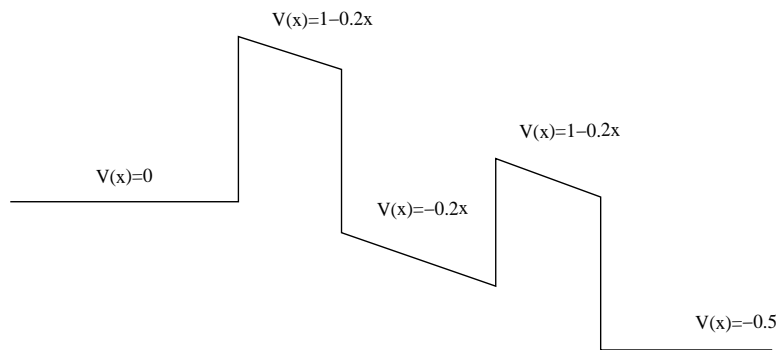
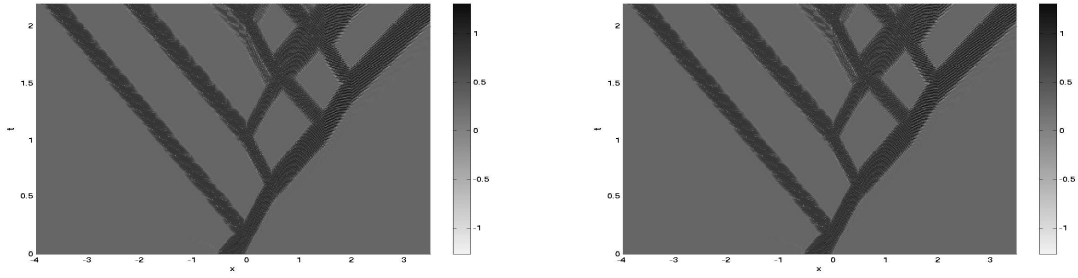
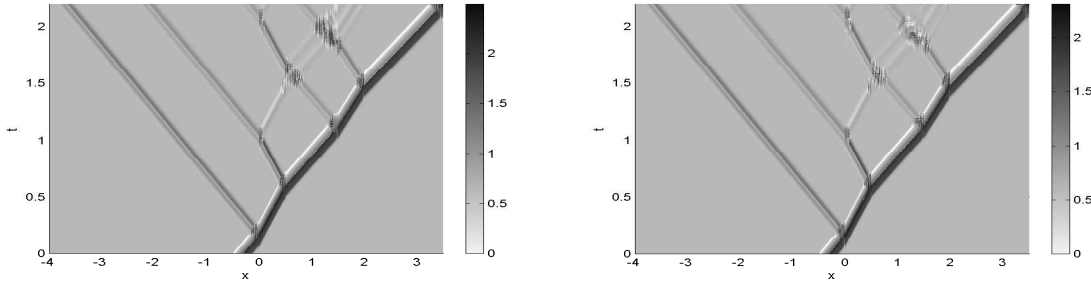


Figure 7: Example 3: An electric potential  $V(x)$  in Resonant Tunneling Diode.

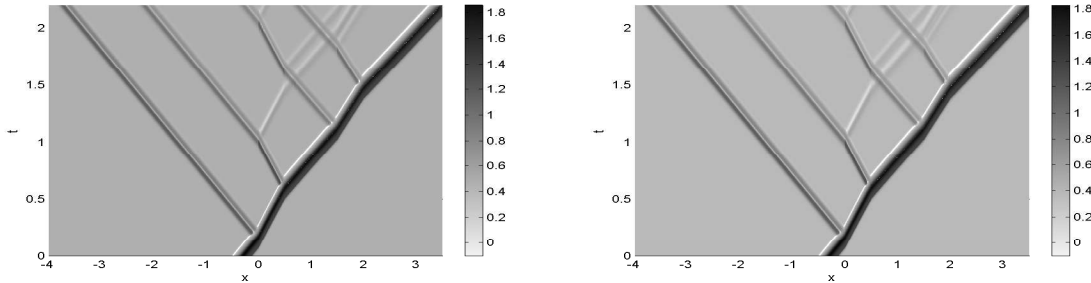
Since  $V(x)$  has a jump at  $x = 0$ , we need the interface conditions for the Gaussian beam method at this interface. In this example, a plan wave propagates from left to right, hits the



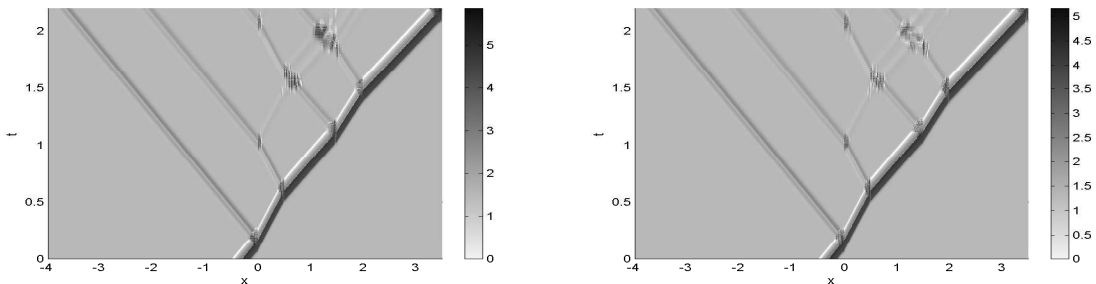
(a) wave function



(b) position density



(c) density flux



(d) kinetic energy

Figure 8: Example 3. Time evolution of the solutions with  $\epsilon = 1/400$ : left, reference solution, right, approximate solution by the Gaussian beam method.

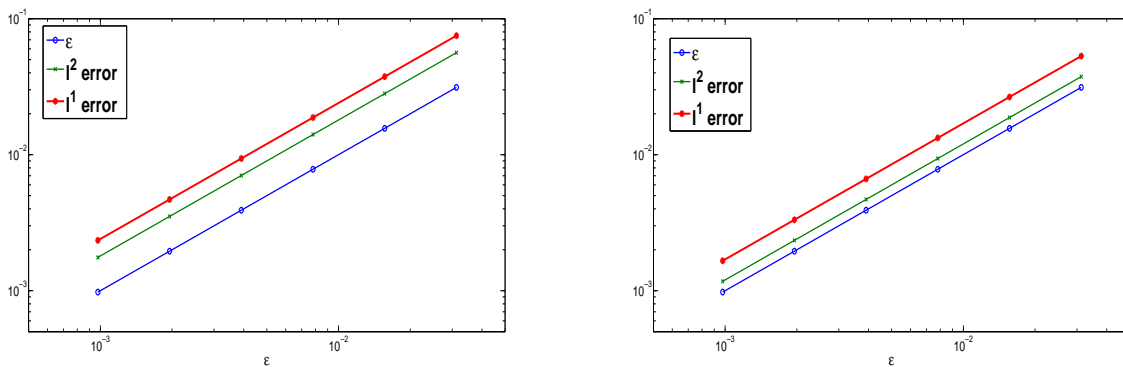


Figure 9: Example 3: the convergence rate with respect to  $\epsilon$  in the  $l^1$  and  $l^2$ -norms, Left, wave function; Right, position density.

interface and gives rise to a reflected wave and a transmitted wave. In our computation, the mesh sizes are chosen as  $\Delta x = \Delta y = \Delta \xi_1 = \Delta \xi_2 = 0.01$ , while  $\Delta t = 1/200$ .

Figure 10(a) shows the wave functions given by a direct simulation using the Schrödinger and by our Gaussian beam solution. Figure 10(b) shows the position density of the exact solution and our Gaussian beam method. Thanks to the interface conditions, our method captures the reflected wave and transmitted wave accurately.

Figure 11(a) and Figure 11(b) give respectively the density fluxes and kinetic energies of the exact solution and the solution of our GB method. Our Gaussian beam method can capture all reflections and transmissions accurately.

**Example 5.5.** *Finally, consider the circular barrier with unit diameter*

$$V(\mathbf{x}) = \begin{cases} 0, & \mathbf{x} \in \Omega_1 = \{\mathbf{x} \mid |\mathbf{x}| > \frac{1}{2}\}, \\ \frac{1}{2}, & \mathbf{x} \in \Omega_2 = \bar{\Omega}_1^c. \end{cases} \quad (5.1)$$

$$A_0(\mathbf{x}) = \frac{4}{\sqrt{2\pi}} \exp\left(-4[(x+1)^2 + (y+1)^2]\right), \quad (5.2)$$

$$S_0(\mathbf{x}) = 0.75x + 0.75y. \quad (5.3)$$

The potential  $V(\mathbf{x})$  is discontinuous at  $|\mathbf{x}| = 1/2$ . The interface is a circle, so the interface conditions for curved interface are needed in the Gaussian beam method. In our computation, the mesh sizes are chosen as  $\Delta x = \Delta y = \Delta \xi_1 = \Delta \xi_2 = 0.005$ , while  $\Delta t = 1/256$ .

Figure 12(a) shows the wave functions given by a direct simulation using the Schrödinger and by our Gaussian beam solution. Figure 12(b) shows the position density of the reference solution and our Gaussian beam method. One can see a good agreement between the two solutions.

Figure 13(a) and Figure 13(b) give respectively the density fluxes and kinetic energies of the exact solution and the solution of our GB method. Our Gaussian beam method can capture all reflections and transmissions accurately.

## 6. CONCLUDING REMARKS

In this paper, we generalize the Gaussian beam methods to solve the Schrödinger equation with discontinuous potentials. Motivated by the Hamiltonian preserving scheme developed in [19], we construct the interface conditions for the reflection and transmission of Gaussian beams. Combining the interface conditions and the decomposition and reinitialization techniques proposed in [40], we obtain the Gaussian beam methods that are able to handle quantum potential barriers. Both 1D and 2D numerical examples are given to verify the accuracy of this method.

In the future, we will extend our method to higher order, and explore its applications to other related problems, such as the quantum tunneling across potential energy levels.

## REFERENCES

- [1] G. Ariel, B. Engquist, N. Tanushev and R. Tsai, Gaussian beam decomposition of high frequency wave fields using expectation-maximization, *Journal of Computational Physics*, 230(6), 2303-2321 (2011)
- [2] W. Bao, S. Jin and P.A. Markowich, On time-splitting spectral approximations for the Schrödinger equation in the semiclassical regime, *J. Comput. Phys.*, 175(2), 487-524 (2002)
- [3] J.D. Benamou, Big ray tracing: multivalued travel time field computation using viscosity solutions of the eikonal equation, *J. Comput. Phys.*, 128, 463-474 (1996)
- [4] L.T. Cheng, H. Liu, and S. Osher, Computational high-frequency wave propagation using the level set method, with applications to the semi-classical limit of Schrödinger equations, *Commun. Math. Sci.*, 1(3), 593C621 (2003)
- [5] L.T. Cheng, M. Kang, S. Osher, H. Shim, Y. Tsai, Reflection in a level set framework for geometric optics, *Comput. Model. Eng. Sci.* 5 (2004) 347-360.
- [6] B. Engquist and O. Runborg, Multi-Phase computations in geometrical optics, *J. Comp. Appl. Math.* 74, 175-192 (1996)
- [7] B. Engquist and O. Runborg, Computational high frequency wave propagation, *Acta Numerica*, 12, 181-266 (2003)
- [8] B. Engquist, O. Runborg and A.K. Tornberg, High frequency wave propagation by the segment projection method, *J. Comput. Phys.*, 178, 373-390 (2002)
- [9] L. Gosse, Using K-branch entropy solutions for multivalued geometric optics computation, *J. Comp. Phys.* 180, 155-182 (2002)
- [10] L. Gosse, S. Jin and X.T. Li, On two moment systems for computing multiphase semiclassical limits of the Schrödinger equation, *Math. Models Meth. Appl. Sci.*, 13(12), 1689-1723 (2003)
- [11] E. J. Heller, Time-dependent approach to semiclassical dynamics, *The Journal of Chemical Physics*, 62(4), 1544-1555 (1975)
- [12] N.R. Hill, Gaussian beam migration, *Geophysics*, 55(11), 1416-1428 (1990)
- [13] N.R. Hill, Prestack Gaussian-beam depth migration, *Geophysics*, 66(4), 1240-1250 (2001)
- [14] S. Jin, P. Markowich and C. Sparber, Mathematical and computational methods for semiclassical Schrödinger equations., *Acta Numerica*, 121-209 (2011)
- [15] S. Jin and K. Novak, A semiclassical transport model for thin quantum barriers, *Multiscale Modeling and Simulation*, 5(4), 1063-1086 (2006)
- [16] S. Jin and X.T. Li, Multi-phase computations of the semiclassical limit of the Schrödinger equation and related problems: Whitham vs. Wigner, *Physica D*, 182, 46-85 (2003)
- [17] S. Jin, H. Liu, S. Osher and R. Tsai, Computing multi-valued physical observables the semi-classical limit of the Schrödinger equations, *J. Comp. Phys.*, 205, 222-241 (2005)
- [18] S. Jin and S. Osher, A level set method for the computation of multivalued solutions to quasi-linear hyperbolic PDEs and Hamilton-Jacobi equations, *Commun. Math. Sci.*, 1(3), 575-591 (2003)

- [19] S. Jin and X. Wen, Hamiltonian-preserving schemes for the Liouville equation with discontinuous potentials, *Commun. Math. Sci.*, 3, 285-315 (2005)
- [20] S. Jin and X. Wen, Hamiltonian-preserving schemes for the Liouville equation of geometrical optics with partial transmissions and reflections, *SIAM J. Num. Anal.* 44, 1801-1828 (2006)
- [21] S. Jin, H. Wu and X. Yang, Gaussian beam methods for the Schrödinger equation in the semi-classical regime: Lagrangian and Eulerian Formulations, *Commun. Math. Sci.*, 6, 995-1020 (2008)
- [22] S. Jin, H. Wu and X. Yang, A numerical study of the Gaussian beam methods for one-dimensional Schrödinger-Poisson equations, *J. Comp. Math.* 28, 261-272 (2010)
- [23] S. Jin, H. Wu and X. Yang, Semi-Eulerian and High Order Gaussian Beam Methods for the Schrodinger Equation in the Semiclassical Regime, *Comm. Comp. Phys.* 9, 668-687 (2011)
- [24] S. Jin, H. Wu, X. Yang and Z. Huang, Bloch Decomposition-Based Gaussian Beam Method for the Schrödinger equation with Periodic Potentials, *J. Comp. Phys.* 229, 4869-4883 (2010)
- [25] J. B. Keller and R. Lewis, Asymptotic methods for partial differential equations: the reduced wave equation and Maxwell's equation, in *Surveys in Applied Mathematics*, eds J.B. Keller, D. McLaughlin and G. Papanicolaou, Plenum Press, New York, 1995.
- [26] S. Leung and J. Qian, Eulerian Gaussian beams for Schrödinger equations in the semi-classical regime, *Journal of Computational Physics*, 228, 2951-2977 (2009)
- [27] S. Leung, J. Qian and R. Burridge, Eulerian Gaussian beams for high-frequency wave propagation, *Geophysics*, 72(5), 61-76 (2007)
- [28] H. Liu, O. Runborg and N. M. Tanushev, Error estimates for Gaussian Beam superpositions, to appear in *Math of Computation*.
- [29] P.A. Markowich, P. Pietra and C. Pohl, Numerical approximation of quadratic observables of Schrödinger-type equations in the semiclassical limit, *Numer. Math.*, 81, 595-630 (1999)
- [30] M. Motamed and O. Runborg, Taylor expansion and discretization errors in Gaussian beam superposition. *Wave Motion*, 47, 421-439 (2010)
- [31] A. Norris, S. White and J. Schrieffer, Gaussian wave packets in inhomogeneous media with curved interfaces, *Proc. R. Soc. Lond. A*, 412, 93-123 (1987)
- [32] M. M. Popov, A new method of computation of wave fields using Gaussian beams, *Wave Motion*, 4, 85-97 (1982)
- [33] J. Qian and L. Ying, Fast Gaussian wavepacket transforms and Gaussian beams for the Schrödinger equation, *J. Comp. Phys.* 229, 7848-7873 (2010)
- [34] J. Ralston, Gaussian beams and the propagation of singularities, *Studies in PDEs*, MAA stud. Math., 23, 206-248 (1982)
- [35] D. Robert, On the Herman-Kluk Semiclassical Approximation, *Reviews in Mathematical Physics*, 22(10), 1123-1145 (2010)
- [36] V. Sverdlov, E. Ungersboeck, H. Kosina, and S. Selberherr. Current transport models for nanoscale semiconductor devices. *Materials Sci. Engin.* 58, 228-270 (2008)
- [37] N. M. Tanushev, B. Engquist and R. Tsai, Gaussian beam decomposition of high frequency wave fields, *J. Comput. Phys.* 228, 8856-8871 (2009)
- [38] N.M. Tanushev, J.L. Qian and J. Ralston, Mountain waves and Gaussian beams, *SIAM Multiscale Modeling and Simulation*, 6, 688-709 (2007)
- [39] N.M. Tanushev, Superpositions and higher order Gaussian beams, *Commun. Math. Sci.*, 6, 449-475 (2008)
- [40] D. Wei, S. Jin, R. Tsai and X. Yang, A level set method for the semiclassical limit of the Schrodinger equation with discontinuous potentials, *J. Comp. Phys.* 229, 7440-7455 (2010)
- [41] W. R. E. Weiss and G. A. Hagedorn, Reflection and transmission of high frequency pulses at an interface, *Transport Theory and Statistical Physics*, 14(5), 539-565 (1985)
- [42] D. Wei and X. Yang, Eulerian Gaussian beam method for high frequency wave propagation in heterogeneous media with discontinuity in one direction, *Comm. Math. Sci.* 10, 1287-1299, 2012.
- [43] X. Wen, High order numerical quadratures to one dimensional delta function integrals, *SIAM, J. Sci. Comput.* 30, 1825-1846 (2008)

- [44] X. Wen, High order numerical methods to two dimensional delta function integrals in level set methods, J. Comput. Phys. 228, 4273-4290 (2009)
- [45] X. Wen, High order numerical methods to three dimensional delta function integrals in level set methods, SIAM, J. Sci. Comput. 32, 1288-1309 (2010)
- [46] D. Yin and C. Zheng, Gaussian beam formulations and interface conditions for the one-dimensional linear Schrödinger equation, Wave Motion, 48, 310-324 (2011)
- [47] D. Yin and C. Zheng, Composite coherent states approximation for one-dimensional multi-phased wave functions, Communications in Computational Physics, 11(3), 951-984 (2012)

(Shi Jin)

DEPARTMENT OF MATHEMATICS, INSTITUTE OF NATURAL SCIENCES  
AND MINISTRY OF EDUCATION KEY LAB FOR SCIENTIFIC ENGINEERING COMPUTING  
SHANGHAI JIAO TONG UNIVERSITY,  
SHANGHAI 200240, P.R. CHINA  
AND DEPARTMENT OF MATHEMATICS  
UNIVERSITY OF WISCONSIN  
MADISON, WI 53706 USA

*E-mail address:* jin@math.wisc.edu

(Dongming Wei)

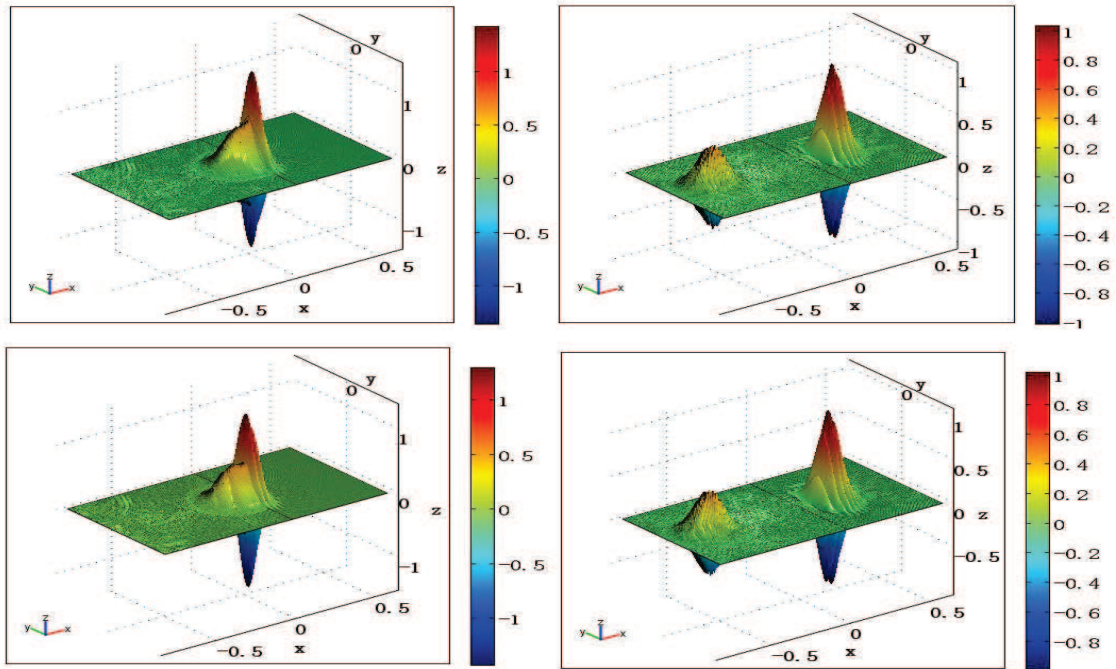
INSTITUTE FOR COMPUTATIONAL AND EXPERIMENTAL RESEARCH IN MATHEMATICS (ICERM)  
BROWN UNIVERSITY  
PROVIDENCE, RI 02912

*E-mail address:* Dongming.Wei@brown.edu

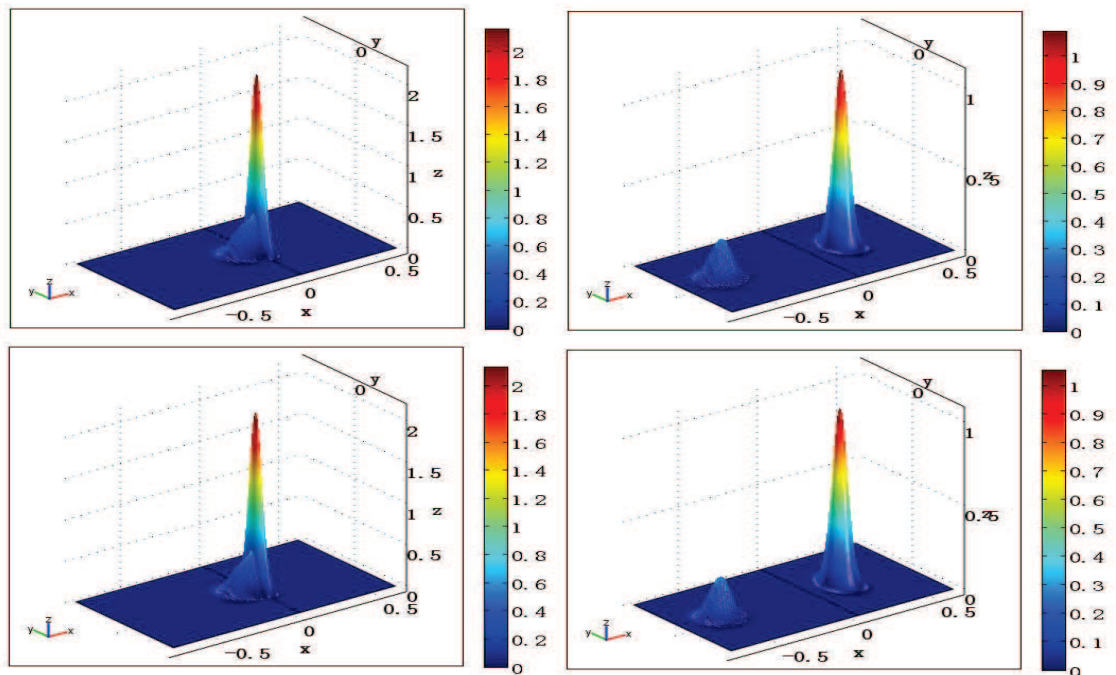
(Dongsheng Yin)

DEPARTMENT OF MATHEMATICAL SCIENCES  
TSINGHUA UNIVERSITY  
BEIJING, 100084, CHINA

*E-mail address:* dyin@math.tsinghua.edu.cn

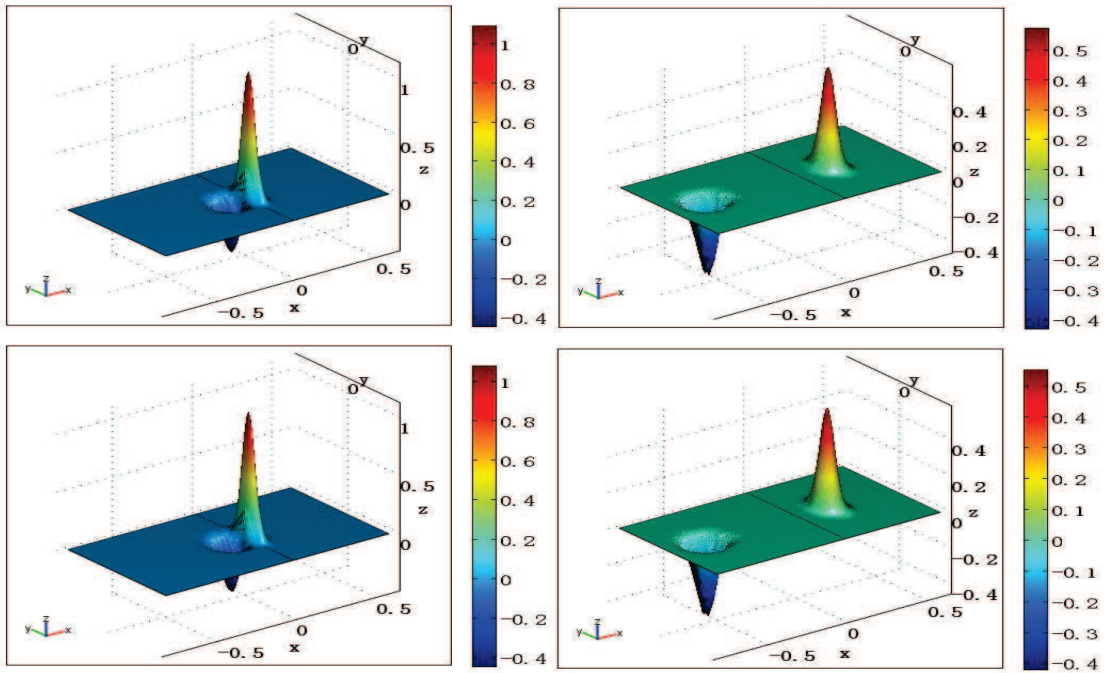


(a) wave function

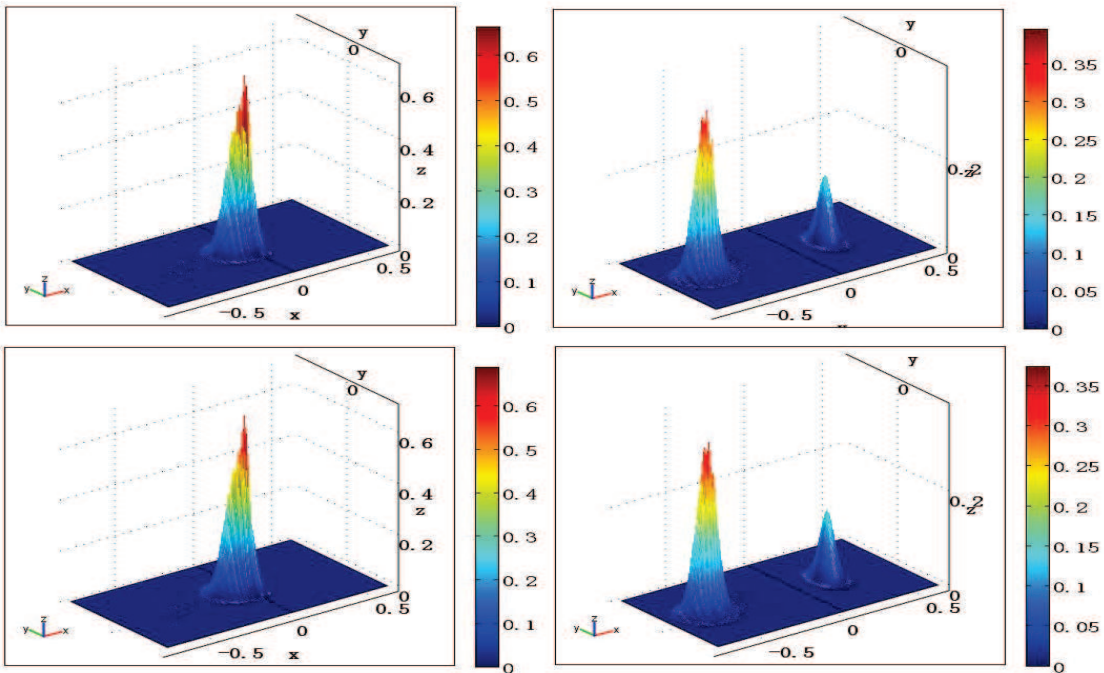


(b) position density

Figure 10: Example 4. Solutions when  $\epsilon = 1/400$ . Left: reference solution; right: approximate solution by our Gaussian beam method. Upper:  $t = 0.32$ , Lower:  $t = 0.64$ .

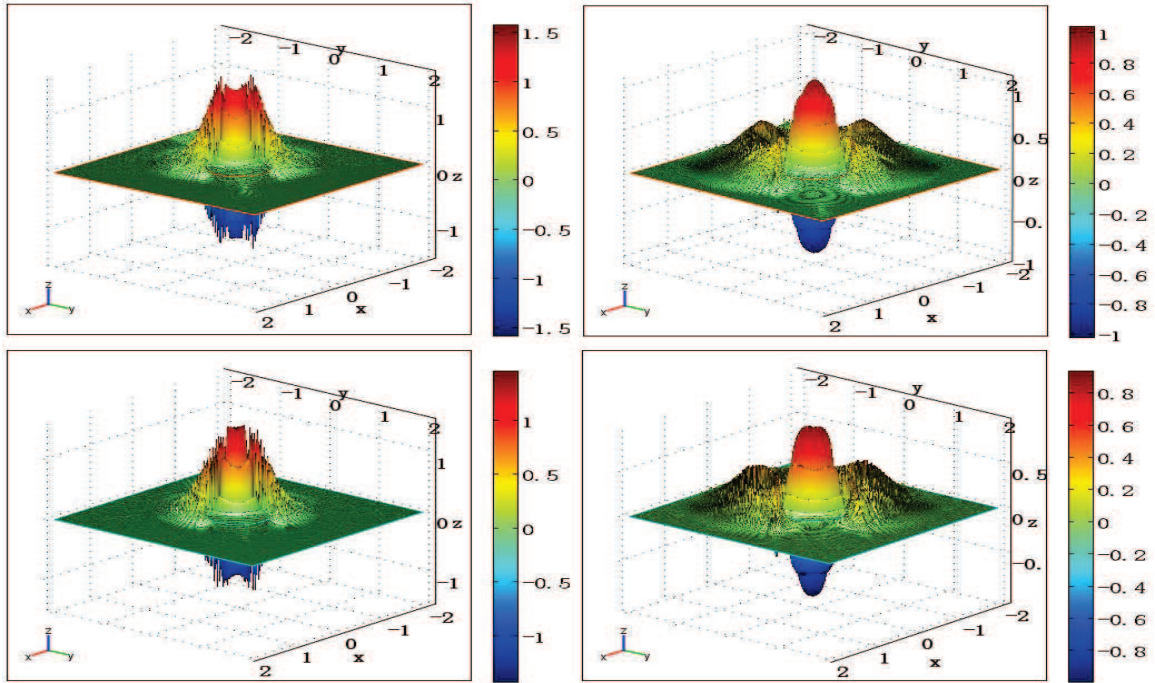


(a) density flux

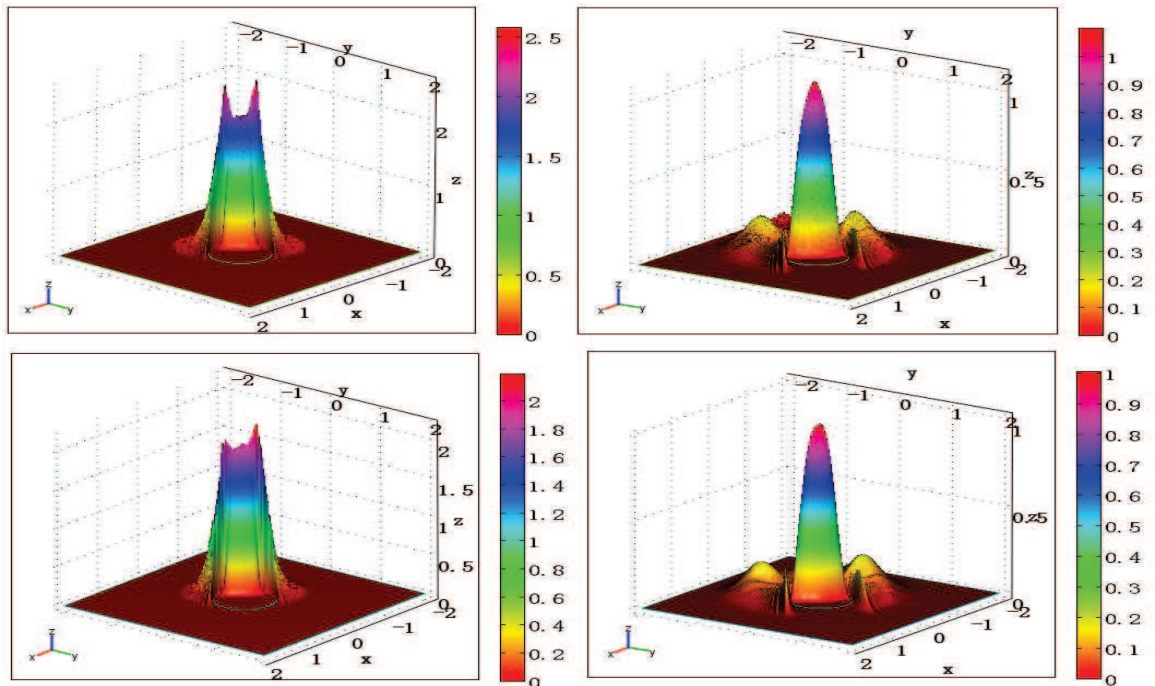


(b) kinetic energy

Figure 11: Example 4. Solutions when  $\epsilon = 1/400$ . Left: reference solution; right: approximate solution by our Gaussian beam method. Upper:  $t = 0.32$ , Lower:  $t = 0.64$ .

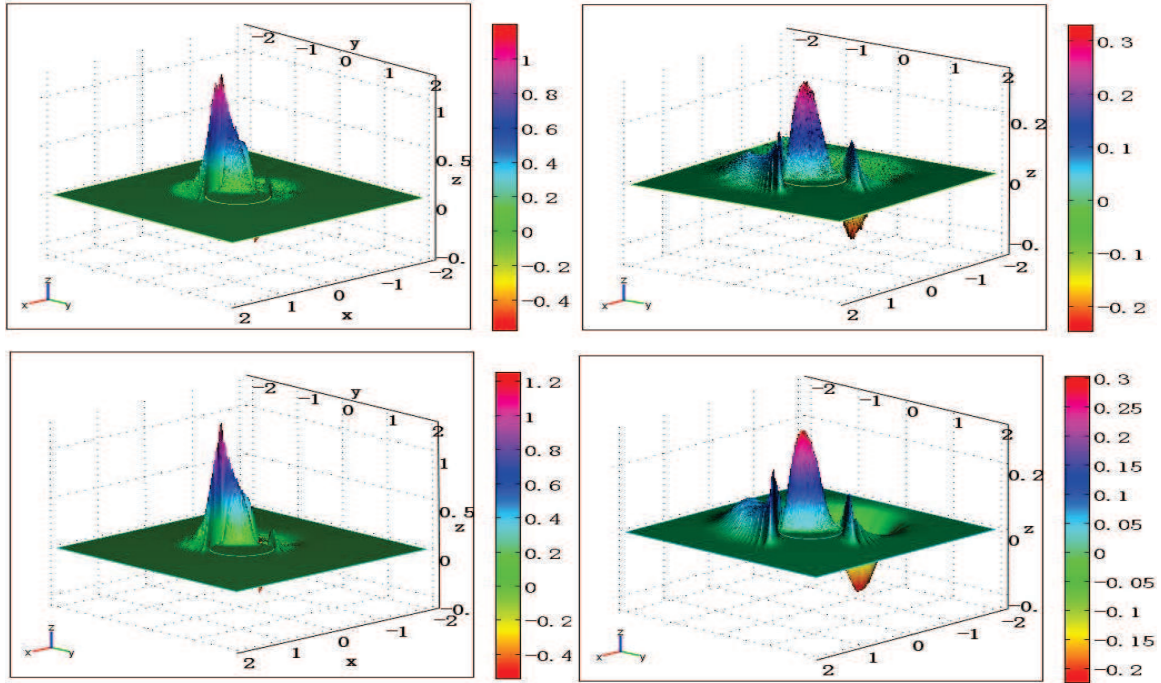


(a) wave function

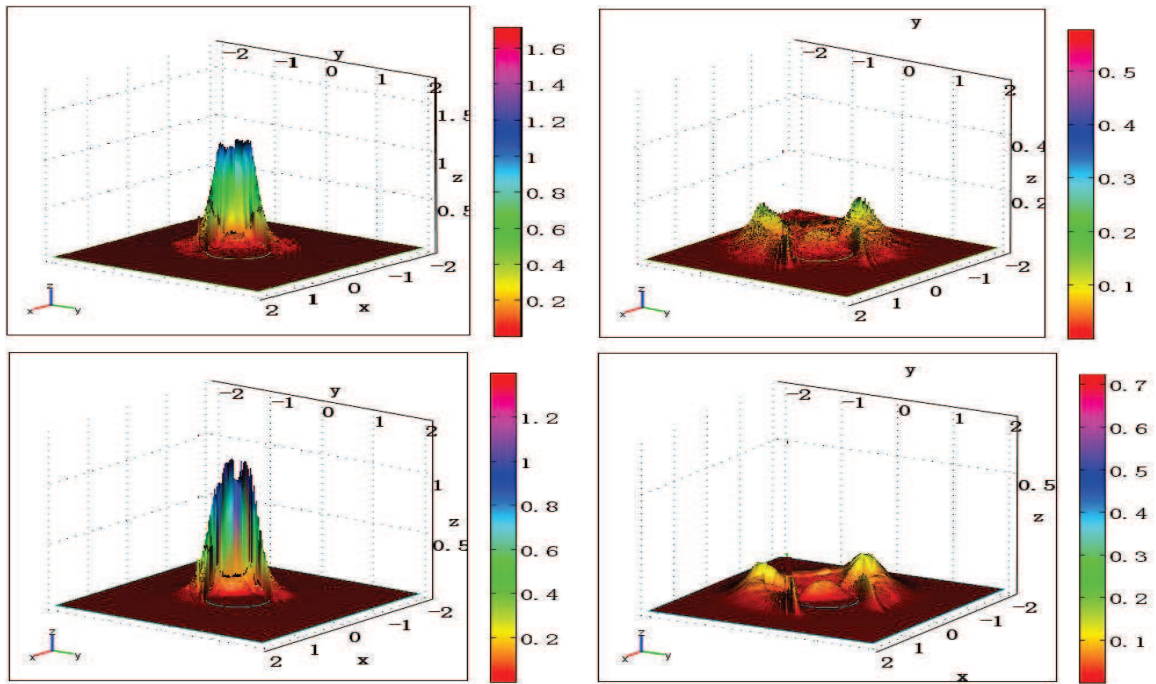


(b) position density

Figure 12: Example 5. Solutions when  $\epsilon = 1/400$ . Left: reference solution; right: approximate solution by our Gaussian beam method. Upper:  $t = 1.0$ , Lower:  $t = 1.6$ .



(a) density flux



(b) kinetic energy

Figure 13: Example 5. Solutions when  $\epsilon = 1/400$ . Left: reference solution; right: approximate solution by our Gaussian beam method. Upper:  $t = 1.0$ , Lower:  $t = 1.6$ .